AD-A065 140 NAVAL OCEAN SYSTEMS CENTER SAN DIEGO CA F/G 9/3
LINEAR PREDICTIVE DIGITAL FILTERING OF NARROWBAND PROCESSES IN --ETC(U)
NOV 78 E H SATORIUS, J R ZEIDLER

UNCLASSIFIED NOSC/TR-331 NL

END
DATE FILMED
4 -79
DDC

LEVEL IV (12)

NOSC

NOSC TR 331

Technical Report 331

LINEAR PREDICTIVE DIGITAL FILTERING OF NARROWBAND PROCESSES IN ADDITIVE BROADBAND NOISE

EH Satorius
JR Zeidler
ST Alexander

1 November 1978

Final Report: FY 1978

Prepared for
Naval Electronic Systems Command

Approved for public release; distribution unlimited.

NAVAL OCEAN SYSTEMS CENTER
SAN DIEGO, CALIFORNIA 92152

NAVAL OCEAN SYSTEMS CENTER, SAN DIEGO, CA 92152

AN ACTIVITY OF THE NAVAL MATERIAL COMMAND

RR GAVAZZI, CAPT, USN
Commander

HL BLOOD
Technical Director

ADMINISTRATIVE INFORMATION

This report was sponsored by the Naval Electronic Systems Command, PME 124-20. The work presented herein was performed during FY 78.

Released by
R. H. Hearn, Head
Electronics Division

Under authority of
D. A. Kunz, Head
Fleet Engineering Department

UNCLASSIFIED

SECURITY CLASSIFICATION OF THIS PAGE (When Data Entered)

REPORT DOCUMENTATION PAGE

READ INSTRUCTIONS BEFORE COMPLETING FORM

1. REPORT NUMBER: NOSC/TR-331
2. GOVT ACCESSION NO.:
3. RECIPIENT'S CATALOG NUMBER:
4. TITLE (and Subtitle): LINEAR PREDICTIVE DIGITAL FILTERING OF NARROWBAND PROCESSES IN ADDITIVE BROADBAND NOISE
5. TYPE OF REPORT & PERIOD COVERED: Final Report FY 78
6. PERFORMING ORG. REPORT NUMBER:
7. AUTHOR(s): E. H. Satorius, J. R. Zeidler, S. T. Alexander
8. CONTRACT OR GRANT NUMBER(s):
9. PERFORMING ORGANIZATION NAME AND ADDRESS: Naval Ocean Systems Center, San Diego, California 92152
10. PROGRAM ELEMENT, PROJECT, TASK AREA & WORK UNIT NUMBERS: 62711N-F11101-XF-111-011-00
11. CONTROLLING OFFICE NAME AND ADDRESS: Naval Electronic Systems Command, Washington, D.C.
12. REPORT DATE: 1 November 1978
13. NUMBER OF PAGES: 53 (12 57p.)
14. MONITORING AGENCY NAME & ADDRESS (if different from Controlling Office): 16 F11101, 17 XF111011
15. SECURITY CLASS. (of this report): Unclassified
15a. DECLASSIFICATION/DOWNGRADING SCHEDULE:

16. DISTRIBUTION STATEMENT (of this Report)

Approved for public release; distribution unlimited.

17. DISTRIBUTION STATEMENT (of the abstract entered in Block 20, if different from Report)

18. SUPPLEMENTARY NOTES

19. KEY WORDS (Continue on reverse side if necessary and identify by block number)

adaptive filtering
Wiener filters
linear prediction

20. ABSTRACT (Continue on reverse side if necessary and identify by block number)

Linear prediction filters (LPF) have recently found a large number of applications in such areas as speech analysis and power spectral estimation. An important application of these filters is to aid the cancellation of additive broadband noise from narrowband signal components. Provided the signal bandwidth is significantly less than the noise bandwidth, the LPF may be used to suppress the additive noise without requiring an external reference noise input (as is required in many noise cancelling applications). The purpose of this report is to provide an analytical basis for bounding the performance of a digital LPF when applied to the problem of cancelling broadband additive noise from narrowband signals. Experimental results obtained with a (continued)

next page

DD FORM 1 JAN 73 1473 EDITION OF 1 NOV 65 IS OBSOLETE S/N 0102-014-6601

UNCLASSIFIED

SECURITY CLASSIFICATION OF THIS PAGE (When Data Entered)

393 159

JOB

20. (Continued) hardware implementation of an adaptive Wiener filter are shown to verify the analytical results.

SUMMARY

Linear prediction filters (LPF) have recently found a large number of applications in such areas as speech analysis and power spectral estimation. An important application of these filters is to aid the cancellation of additive broadband noise from narrowband signal components. Provided the signal bandwidth is significantly less than the noise bandwidth, the LPF may be used to suppress the additive noise without requiring an external reference noise input (as is required in many noise cancelling applications). The purpose of this report is to provide an analytical basis for bounding the performance of a digital LPF when applied to the problem of cancelling broadband additive noise from narrowband signals. Experimental results obtained with a hardware implementation of an adaptive Wiener filter are shown to verify the analytical results.

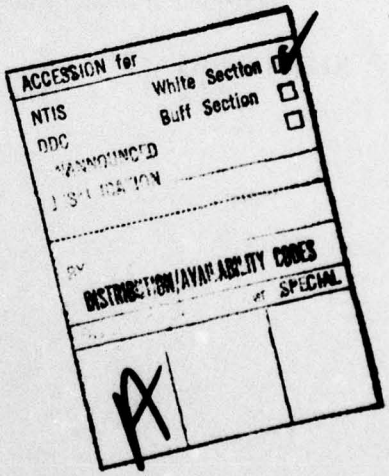

CONTENTS

I. Introduction. . . Page 3

II. Properties of the Digital Wiener Prediction Filter for Inputs with Rational Power Spectra. . . 5

III. LPF Analysis for Inputs Consisting of Narrowband Processes and Additive Broadband Noise. . . 8

IV. Hardware Simulations of an Adaptive Implementation of an LPF. . . 23

V. Conclusions. . . 27

APPENDIX A. General form of the Discrete LPF for Stationary Inputs with Rational Power Spectrum Representations. . . 29

APPENDIX B. Derivation of the Coefficient Equations for the $B_m^{\pm}$ and $C_r^{\pm}$. . . 33

APPENDIX C. Development of Approximate Pole-Zero Models for Narrowband Processes in Additive Broadband Noise. . . 39

APPENDIX D. Treatment of the Coefficient Equations for Narrowband Processes Embedded in Broadband Noise. . . 44

REFERENCES. . . 51

I. INTRODUCTION

Frequently it is of interest to digitally filter out narrowband signals which are embedded in additive broadband noise. This filtering can often be accomplished using fixed bandpass digital filters (e.g., [1]) provided the center frequencies of the signals and their bandwidths are known, a priori, and do not change with time. In many cases of practical interest, however, such a priori information does not exist and alternate filtering schemes must be employed.

When the signals and noise can be considered as random processes with given cross-correlation and autocorrelation functions, Wiener filtering techniques are often effective. The design of Wiener filters requires that the signal and noise be stationary and that the various crosscorrelation and autocorrelation functions be known a priori [2]. Wiener filters have a wide range of applications, however, because the required statistics may be estimated directly from the data thereby alleviating the need for a priori knowledge of such parameters as the signal frequencies.

The design of adaptive filters which continuously estimate the Wiener filter coefficients has been considered by a number of authors. The various adaptive estimation techniques include the pioneering work of Widrow who developed the least mean square (LMS) adaptive filter in References [3–5] which employs a noisy gradient algorithm. Alternatives to the LMS algorithm have also been developed in References [6–10] and a more complete discussion of some of the various adaptive implementations of Wiener filters and their applications is given in Reference [11]. It should be noted that adaptive Wiener filters have found a number of noise cancellation applications in such areas as medicine [5], adaptive line enhancement [12, 29], and speech processing [13]. Other areas of application of adaptive Wiener filters include predictive deconvolution [37], acoustic Doppler extraction [38], and real time linear prediction [36].

In many applications of Wiener filtering to noise cancellation, an external reference input is used [5]. This external reference input should consist of noise which is uncorrelated with the signal and highly correlated with the additive noise corruption in order for the Wiener filter to effectively cancel the additive noise. In applications where an external reference for the additive noise is not available, it is possible to cancel the additive noise using a Wiener linear prediction filter (LPF) if the signal bandwidth is significantly less than the bandwidth of the additive noise.

A schematic diagram of a finite impulse response (FIR) Wiener LPF is illustrated in Figure 1. The impulse response, $w^*(k)$ $(k = 0, \ldots, L-1)$, is chosen to minimize the power in the error signal $\epsilon(j)$, and the delay, Δ, represents the prediction distance of the filter. The noise suppression capabilities of the discrete LPF arise from the fact that the decorrelation time for broadband noise is smaller than that for the narrowband signals. Therefore, it may be possible to choose a value for Δ which will effectively decorrelate the broadband noise and prevent the noise components from appearing in the LPF output (y(j) in Figure 1).

The application of LPF techniques to noise suppression presents a number of fundamental questions regarding, e.g., the values of Δ and L required for the maximum amount of noise reduction without appreciable signal distortion. The elimination of signal distortion is particularly relevant to the application of LPF methods to speech enhancement [13]. This report will provide an analytical basis for bounding the performance of digital linear prediction filters for input data consisting of narrowband signals embedded in additive broadband

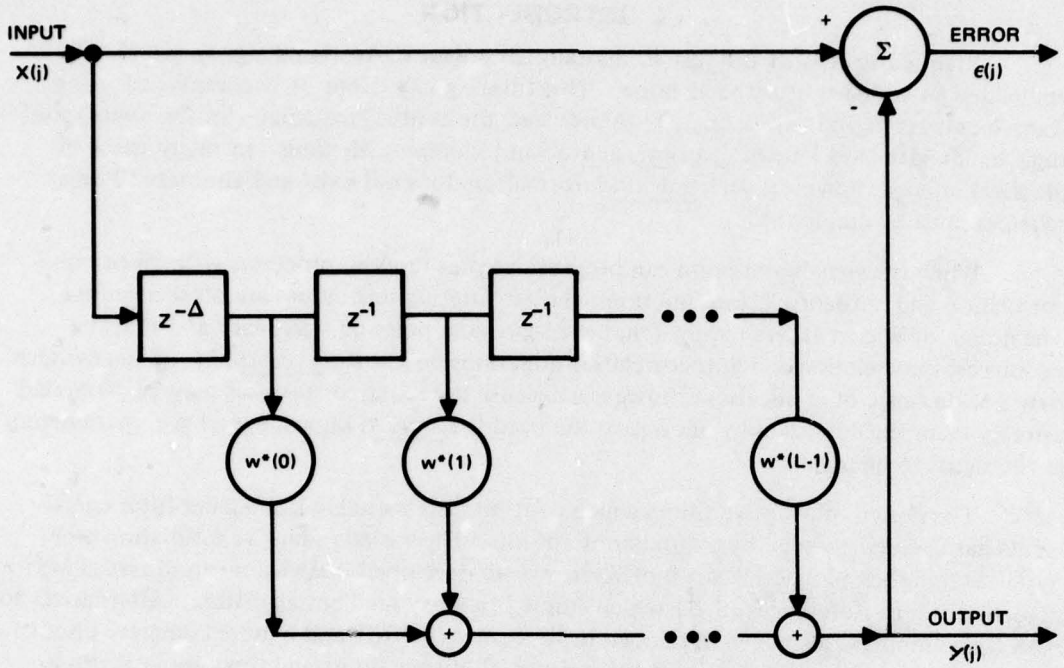

Figure 1. Linear prediction Wiener filter.

noise. Specifically, the impulse response and transfer function of a theoretical, discrete Wiener LPF will be examined.†

Analytic expressions for the LPF impulse response when the input sequence, x(j), is stationary and the z-transform of the autocorrelation function of x is a rational function of z will be developed in Section II. The special case of narrowband signals embedded in additive broadband noise will be treated in detail in Section III. Specifically, a rational spectral density model will first be developed to approximate the power spectrum of the narrowband signals plus noise. Then, using the results of Section II, the discrete LPF impulse response will be derived. The limiting cases of all pole noise (no signals) and sinusoids in additive noise will be examined.†† Finally, in Section IV, results of experimental simulations of an adaptive implementation of the LPF will be presented and discussed.

---

†It will be assumed that the autocorrelation function of the LPF input (x(j) in Figure 1) is known exactly. Therefore, questions regarding specific implementations of an LPF (adaptive or otherwise) will not be addressed in this report.

††Another interesting special case, which is amenable to detailed analysis occurs when the input spectrum contains a notch. This case is discussed in [24].

II. PROPERTIES OF THE DIGITAL WIENER PREDICTION FILTER FOR INPUTS WITH RATIONAL POWER SPECTRA

The properties of the LPF structure discussed in this section are derived using discrete Wiener filter theory [14–16]. A number of other interesting properties of linear prediction filters, a discussion of their applications to a number of different fields, and an extensive bibliography can be found in the excellent review articles by Makhoul [17] and Kailath [18], as well as in the book by Markel and Gray [34].

Referring to Figure 1, the Wiener filter coefficients, $w^*(k)$ ($k = 0, 1, \ldots, L-1$), which minimize the power in the error sequence, $\epsilon(j)$, satisfy the following set of linear equations (e.g., [17, 20]):

$$\sum_{k=0}^{L-1} \phi_{xx}(\ell - k)\, w^*(k) = \phi_{xx}(\ell + \Delta) \qquad \ell = 0, 1, \ldots, L-1, \tag{1}$$

where $\phi_{xx}(k)$ represents the discrete autocorrelation function of $x(j)$ and is given by $\phi_{xx}(k) = E[x(j)\, x(j+k)]$ where $E[\cdot]$ denotes expectation. Equation (1) represents the discrete analog of the integral equation derived in Reference [19] for the continuous, finite duration Wiener filter.

Our analysis will be restricted to the case when the z transform of $\phi_{xx}(k)$, i.e.,

$$S_{xx}(z) \equiv \sum_{k=-\infty}^{\infty} \phi_{xx}(k)\, z^{-k}, \tag{2}$$

is a rational function of z. There are two reasons for this. First, for this important case, Eq. (1) can be solved by elementary methods and its solution provides insight into the analytic structure of the LPF. Second, the special case of $S_{xx}(z)$ being rational provides a good description of a much broader class of stationary random inputs since any analytic function may be closely approximated by a rational function. In particular, as will be discussed in the next section, relatively simple rational power spectrum models can be developed to describe an important class of inputs, i.e., narrowband signals and additive broadband noise.

Therefore, we shall write $S_{xx}(z)$ as

$$S_{xx}(z) = A \frac{\prod_{m=1}^{M} (z - e^{-\mu_m + j\theta_m})(z^{-1} - e^{-\mu_m - j\theta_m})}{\prod_{n=1}^{N} (z - e^{-\alpha_n + j\omega_n})(z^{-1} - e^{-\alpha_n - j\omega_n})}, \tag{3}$$

where the μ_m and α_n are non-zero, positive real constants and

$$-\pi \leq \omega_n, \theta_m \leq \pi, \text{ for all m, n.}$$

Also, in Eq. (3) A is a real, positive constant and an overbar denotes complex conjugation. The expansion in Eq. (3) with $z = \exp(j\omega)$ ($-\pi \leq \omega \leq \pi$) represents the power spectrum of a

complex process. For a real process, the zeroes and poles of $S_{xx}(z)$ will either be real or appear in complex conjugate pairs. Therefore, the expansion in Eq. (3) is more general than that for a real process and will prove useful in the later sections.†

In this report, we will explicitly treat the case of $M \leq N$. The case of $M > N$ can be treated by a straightforward extension of the methods discussed here. As shown in Appendices A and B, when $M < N$, $w^*(k)$ can be represented as follows [Appendix A, Eq. (A-19)]:

$$w^*(k) = \sum_{m=1}^{M} \left\{ B_m^+ e^{-\mu_m k + j\theta_m k} + B_m^- e^{-\mu_m (L-1-k) + j\theta_m k} \right\}$$

$$+ \sum_{r=1}^{N-M} \left\{ C_r^+ \delta(k - r + 1) + C_r^- \delta(k + r - L) \right\} \qquad k = 0, 1, \ldots, L-1, \qquad (4)$$

where $\delta(k)$ is the Kronecker delta function, i.e., $\delta(k) = 0$ for $k \neq 0$ and $\delta(0) = 1$. The constants $B_m^{\pm}$ and $C_r^{\pm}$ may be obtained by solving the following set of linear equations [Appendix B, Eq. (B-12)].

$$\sum_{m=1}^{M} \left\{ \frac{B_m^+}{1 - e^{\alpha_n - \mu_m - j(\omega_n - \theta_m)}} + \frac{B_m^- e^{-\mu_m (L-1)}}{1 - e^{\alpha_n + \mu_m - j(\omega_n - \theta_m)}} \right\}$$

$$+ \sum_{r=1}^{N-M} C_r^+ e^{\alpha_n (r-1) - j\omega_n (r-1)} = e^{-\alpha_n \Delta + j\omega_n \Delta} \qquad n = 1, \ldots, N; \qquad (5)$$

and,

$$\sum_{m=1}^{M} \left\{ \frac{B_m^+ e^{-\mu_m L + j\theta_m L}}{1 - e^{-\alpha_n - \mu_m - j(\omega_n - \theta_m)}} + \frac{B_m^- e^{\mu_m + j\theta_m L}}{1 - e^{-\alpha_n + \mu_m - j(\omega_n - \theta_m)}} \right\}$$

$$- \sum_{r=1}^{N-M} C_r^- e^{\alpha_n r + j\omega_n r} = 0 \qquad n = 1, \ldots, N. \qquad (6)$$

The solution of Eqs. (5) and (6), together with (4) provides the complete solution for $w^*(k)$ when $M < N$. The only modification which is needed when $M = N$ is to remove the summation terms involving the delta functions in Eq. (4) and the summation terms involving the $C_r^{\pm}$ in Eqs. (5) and (6). That is, when $M = N$ only damped exponentials appear in the analytic solution for the LPF coefficients, $w^*(k)$.

A number of interesting properties of the FIR linear prediction filter may be noted from Eqs. (4) through (6). First, it is seen from Eq. (4) that $w^*(k)$ consists of sums of damped exponentials, $\exp(\pm\mu_m k + j\theta_m k)$, as well as impulses. It is further seen that the exponentials, which are the zeroes of $S_{xx}(z)$, decay away from each end of the filter with the

---

†It should be noted that if x(j) is a complex process, then $w^*(k)$ will still be given by (1) but $\phi_{xx}(k)$ would be given by: $\phi_{xx}(k) = E[\overline{x(j)}\, x(j+k)]$.

B_m^+ and B_m^- representing the amplitudes of the damped exponentials which decay from the beginning and end of the filter, respectively. Likewise, the C_r^+ and C_r^- represent the amplitudes of the impulses which occur at the beginning and end of the filter, respectively. Therefore, the constants associated with the "–" superscripts can be thought of as reflection amplitudes which are the direct result of the finite filter length. From Eq. (5) it is seen that the B_m^- couple into the N equations for the B_m^+ and C_r^+ through coupling coefficients which are proportional to exp $(-\mu_m L)$. Vice versa, from Eq. (6) it is seen that the B_m^+ couple into the N equations for the B_m^- and C_r^- (the reflection amplitudes) through coupling coefficients which are also proportional to exp $(-\mu_m L)$. As $L \to \infty$, these coupling coefficients approach zero and from (6), the reflection amplitudes, B_m^- and C_r^- also approach zero. Therefore, as $L \to \infty$, i.e., as exp $(-\mu_m L) \to 0$, the reflection amplitudes approach zero and $w^*(k)$ can be represented as a sum of damped exponentials and impulses all of which occur at the beginning of the filter. It should be noted that the reflection amplitudes, B_m^- and C_r^-, are similar to the reflection coefficients, K_m, which appear in the Levinson-Durbin algorithm [17]. In fact, the K_m may be related to all the amplitudes, $B_m^\pm$ and $C_r^\pm$, through the relation [17]:

$$K_p = w^*(p), \tag{7}$$

with $p = L - 1$ in Eq. (4). As is the case with the reflection amplitudes, it is seen from Eqs. (4) through (7) that the reflection coefficients also decay to zero as the filter length becomes infinite.

Equation (4) also enables one to write an explicit relation for the frequency response, $H_L^*(\omega)$, of the discrete LPF in terms of the $B_m^\pm$, $C_r^\pm$:

$$H_L^*(\omega) \equiv \sum_{k=0}^{L-1} w^*(k)\, e^{-j\omega(k+1)} = e^{-j\omega} \sum_{m=1}^{M} \left\{ B_m^+ \frac{1 - e^{-\mu_m L + j(\theta_m - \omega)L}}{1 - e^{-\mu_m + j(\theta_m - \omega)}} \right.$$

$$\left. + B_m^-\, e^{-\mu_m (L-1)} \frac{1 - e^{(\mu_m + j(\theta_m - \omega))L}}{1 - e^{(\mu_m + j(\theta_m - \omega))}} \right\}$$

$$+ e^{-j\omega} \sum_{r=1}^{N-M} \left\{ C_r^+\, e^{-j\omega(r-1)} + C_r^-\, e^{-j\omega(L-r)} \right\}. \tag{8}$$

As $\mu_m L \to \infty$, B_m^-, C_r^-, and exp $(-\mu_m L) \to 0$ and $H_L^*(\omega)$ approaches:

$$\lim_{L \to \infty} H_L^*(\omega) \equiv H_\infty^*(\omega) = \sum_{m=1}^{M} \frac{B_m^+\, e^{-j\omega}}{1 - e^{-\mu_m + j(\theta_m - \omega)}}$$

$$+ \sum_{r=1}^{N-M} C_r^+\, e^{-j\omega r}. \tag{9}$$

Note that from Eq. (9), $|H_\infty^*(\omega)|$ will tend to have peaks at the angular frequencies, θ_m, of the zeroes of $S_{xx}(z)$. This result is consistent with the "whitening" filter interpretation of an LPF (with $\Delta = 1$). This interpretation (e.g., [17], [18], [23]) states that as L becomes large, the power spectrum of the LPF error output, $e(j)$ in Figure 1, will become approximately flat

when $\Delta = 1$. Therefore, since the input spectrum has depressions at the angular frequencies of the zeroes of $S_{xx}(z)$, then the magnitude squared of the transfer function between ϵ and x, i.e., $|1 - H_L^*(\omega)|^2$, should have peaks at the angular frequencies of the zeroes of $S_{xx}(z)$. This, of course, implies that $|H_L^*(\omega)|$ will also tend to have peaks at the angular frequencies of the zeroes of $S_{xx}(z)$. It should be pointed out that although the "whitening" filter argument only applies when $\Delta = 1$, it does provide an indication of the behavior of $|H_L^*(\omega)|$ near the angular frequencies of the zeroes of $S_{xx}(z)$ even when $\Delta > 1$. (Indeed, Δ only enters into the expression for $|H_L^*(\omega)|$ through the scaling factors, $e^{-\alpha_n \Delta + j\omega_n \Delta}$, which appear on the right-hand side of Eq. (5).) When $\Delta = 1$ and $\mu_m L \approx 0$ (for any m), the LPF cannot completely whiten the input spectrum due to the interaction between the "+" and "–" coefficients in Eqs. (5) and (6).

Equations (4) through (9) provide a simplified method for obtaining $w^*(k)$ and $H_L^*(\omega)$ in terms of the poles and zeroes of $S_{xx}(z)$. (Note that the dimensionality of these equations is determined by N and M and is independent of L and Δ.) For many applications this formulation allows L and Δ to be treated as adjustable design parameters which can be optimized on the basis of desired performance criteria (e.g., [12], [21]). One of the main difficulties in applying the above results is obtaining an appropriate, simple pole-zero model for the input. This particular problem will be addressed in the next section.

III. LPF ANALYSIS FOR INPUTS CONSISTING OF NARROWBAND PROCESSES AND ADDITIVE BROADBAND NOISE

DETERMINATION OF APPROPRIATE POLE-ZERO MODELS FOR NARROWBAND PROCESSES IN ADDITIVE BROADBAND NOISE

A representative model for a sum of bandpass processes embedded in additive broadband noise may be expressed by the following autocorrelation function:

$$\phi_{xx}(k) = \phi_{no}(k) + \sum_{n=1}^{N} \sigma_n^2 e^{-\alpha_n |k|} \cos \omega_n k. \tag{10}$$

In Eq. (10), σ_n^2, α_n, and ω_n represent the power, 3-dB half bandwidth, and frequency, respectively, of the n^{th} signal and $\phi_{no}(k)$ represents the autocorrelation function for the background additive noise. We will assume that the z-transform of $\phi_{no}(k)$, $S_{no}(z)$, can be expressed as a rational function of z, i.e.,

$$S_{no}(z) = \sigma_{no}^2 \frac{\prod_{m=1}^{M_o} (z - e^{-\mu'_m + j\theta'_m})(z^{-1} - e^{-\mu'_m - j\theta'_m})}{\prod_{n=1}^{N_o} (z - e^{-\alpha'_n + j\omega'_n})(z^{-1} - e^{-\alpha'_n - j\omega'_n})}, \tag{11}$$

where, as in the case of Eq. (3), the μ'_m and α'_n are non-zero, positive real constants and

$$-\pi \leq \omega'_n, \theta'_m \leq \pi, \text{ for all m,n.}$$

Also, in Eq. (11), σ^2_{no} is a real positive constant and it will be assumed that $M_o \leq N_o$.

Note that for large k, $\phi_{no}(k)$ will consist of sums of damped exponentials with magnitudes decaying as $e^{-\alpha'_n k}$. Therefore, the assumption that the decorrelation interval for the broadband noise is much smaller than that for the narrowband processes is equivalent to requiring that

$$1/\alpha'_{min} \ll \frac{1}{\alpha_n} \qquad n = 1, 2, \ldots, N, \tag{12}$$

where α'_{min} denotes the smallest of all the α'_n ($n = 1, 2, \ldots, N_o$). It is this property of broadband noise and narrowband signals which may be exploited when choosing a value for Δ as will be discussed later.

As shown in the previous section, once the zeroes and poles of $S_{xx}(z)$ are known, the $w^*(k)$ and $H^*_L(\omega)$ can be determined through Eqs. (4) through (6) and (8). Although the poles of $S_{xx}(z)$ are simply the poles of $S_{no}(z)$ as well as those obtained from the 2N signal poles (i.e., $\exp(\pm\alpha_n \pm j\omega_n)$ ($n = 1, 2, \ldots, N$)), the zeroes of $S_{xx}(z)$ do not have a simple analytic form (except for special cases involving small values of N, M_o, and N_o). However, when the α_n are all much smaller than unity so that the background noise spectral density may be closely approximated from $S_{xx}(e^{j\omega})$ ($\omega \neq \omega_n$) (i.e., no appreciable overlap of signal spectra), then a simple approximating expression for the zeroes may be derived.

The details of this approximation are given in Appendix C. The resulting approximate expressions for the zeroes are given by (Appendix C, Eq. (C-20)):

$$e^{\pm\mu'_m + j\theta'_m}, \qquad m = 1, \ldots, M_o \tag{13a}$$

and

$$e^{\pm\beta_n + j\psi_n}, \qquad n = 1, \ldots, 2N$$

where

$$\beta_n = \cosh^{-1}\left\{\cosh\alpha_n + \frac{1}{2}\,SNR_n \sinh\alpha_n\right\}$$

and

$$\beta_{n+N} = \beta_n \text{ for } n = 1, \ldots, N \tag{13b}$$

$$\psi_n = \omega_n \text{ and } \psi_{n+N} = -\omega_n \qquad n = 1, \ldots, N. \tag{13c}$$

In Eq. (13), $SNR_n \equiv \sigma^2_n / S_{no}(e^{j\omega_n})$ and is the signal-to-noise spectral density ratio (SNR) at the n^{th} signal. It should be noted that for small α_n, β_n in (13b) may be further approximated by:

$$\beta_n = \sqrt{\alpha_n^2 + SNR_n\,\alpha_n}\,. \tag{14}$$

Equations (13a) through (13c) show that as the α_n approach zero, the zeroes of $S_{xx}(z)$ can be approximated by the M_o zeroes of $S_{no}(z)$ and the zeroes due to the narrowband signals. These signal zeroes are displaced slightly back along radial lines from the signal pole locations. As the signal bandwidths approach zero, both the signal zeroes and poles approach the unit circle. However, the signal poles approach the unit circle faster (as a function of the α_n) than the signal zeroes, i.e., we have from Eq. (14) (or (13b)) that:

$$\beta_n \approx \sqrt{SNR_n\, \alpha_n}, \tag{15}$$

as

$$\alpha_n \to 0 \ (SNR_n \text{ fixed}).$$

Also, from Eq. (13), as the signal powers approach zero, the signal zeroes cover the signal poles and $S_{xx}(z)$ reduces to $S_{no}(z)$ as it should.

To obtain a better feeling for the approximations involved in Eq. (13), plots are presented in Figures 2 through 5 of $S_{xx}(e^{j\omega})$ $(-\pi \leq \omega \leq \pi)$ computed exactly and computed approximately using Eq. (13) for two narrowband signals embedded in broadband noise. In the cases selected, the autocorrelation function of the signals is given by

$$\sigma_1^2\, e^{-\alpha_1 |k|} \cos 2\pi f_1 k + \sigma_2^2\, e^{-\alpha_2 |k|} \cos 2\pi f_2 k,$$

and the autocorrelation function of the noise is given by

$$P_0 \delta(k) + P_1 e^{-\alpha_0 |k|}.$$

In Figures 2 through 5, $\sigma_1^2 = \sigma_2^2 = 1.0$, $P_0 = 5.0$, $f_1 = 0.125$, $f_2 = 0.375$, $\alpha_1 = 0.05$, and α_0, α_2, and P_1 are variable. As is seen in these figures, Eq. (13) provides a very good approximation to the true zeroes of the input power spectrum. In fact, in Figures 2 through 4, the exact and approximate curves lie on top of each other. The only noticeable difference occurs in Figure 5 in the vicinity of the lower signal frequency $f_1 = 0.125$ where the background noise spectral density is not flat. As noted in Appendix C (C-19), the approximations expressed by Eq. (13) become worse when the spectral density of the noise varies considerably in the vicinity of the signal.

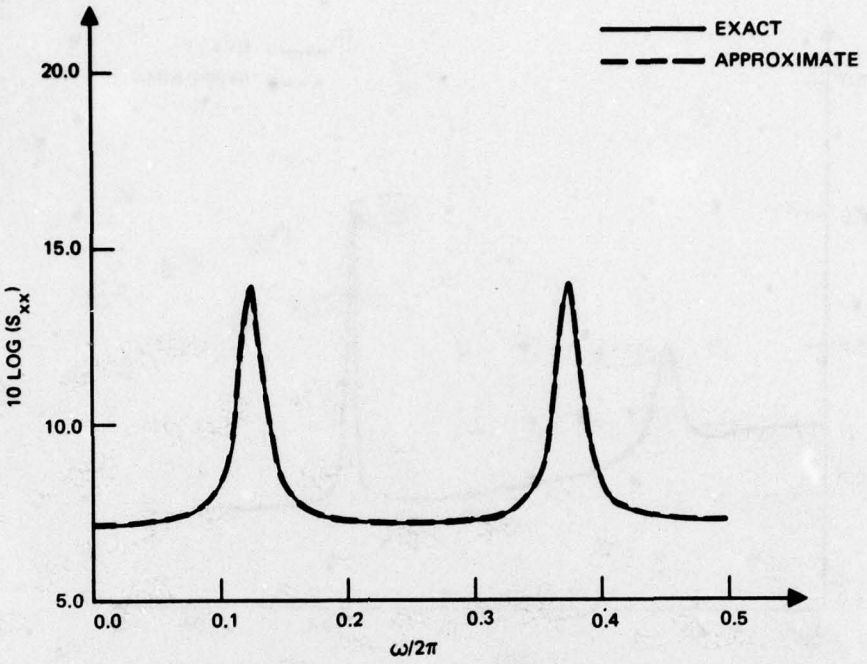

Figure 2. Exact and approximate plots of $S_{xx}(e^{j\omega})$ (in dB) for $\sigma_1^2 = \sigma_2^2 = 1.0$; $P_0 = 5.0$; $P_1 = 0$; $\alpha_1 = \alpha_2 = 0.05$; $f_1 = 0.125$; and $f_2 = 0.375$.

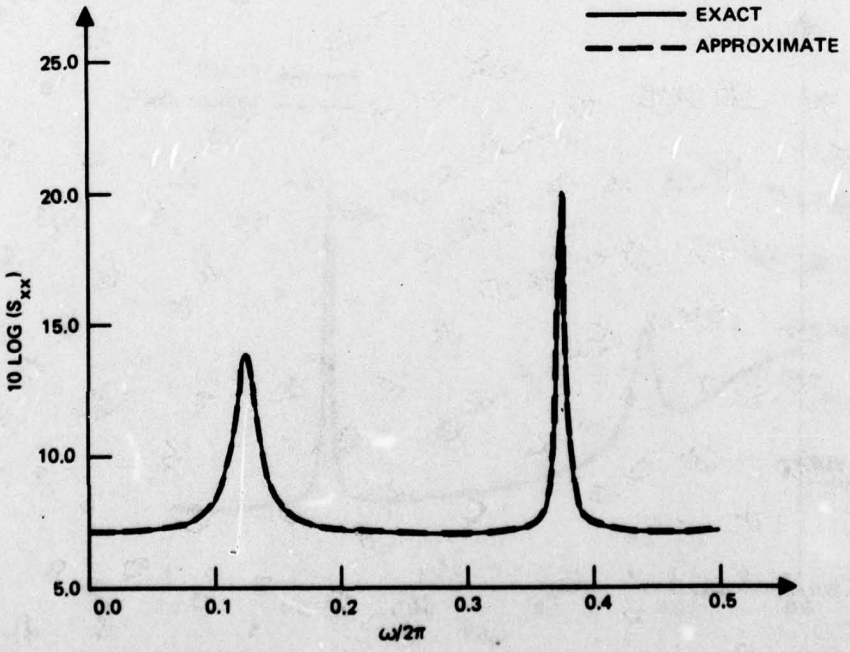

Figure 3. Exact and approximate plots of $S_{xx}(e^{j\omega})$ (in dB) for $\sigma_1^2 = \sigma_2^2 = 1.0$; $P_0 = 5.0$; $P_1 = 0$; $\alpha_1 = 0.05$; $\alpha_2 = 0.01$; $f_1 = 0.125$; and $f_2 = 0.375$.

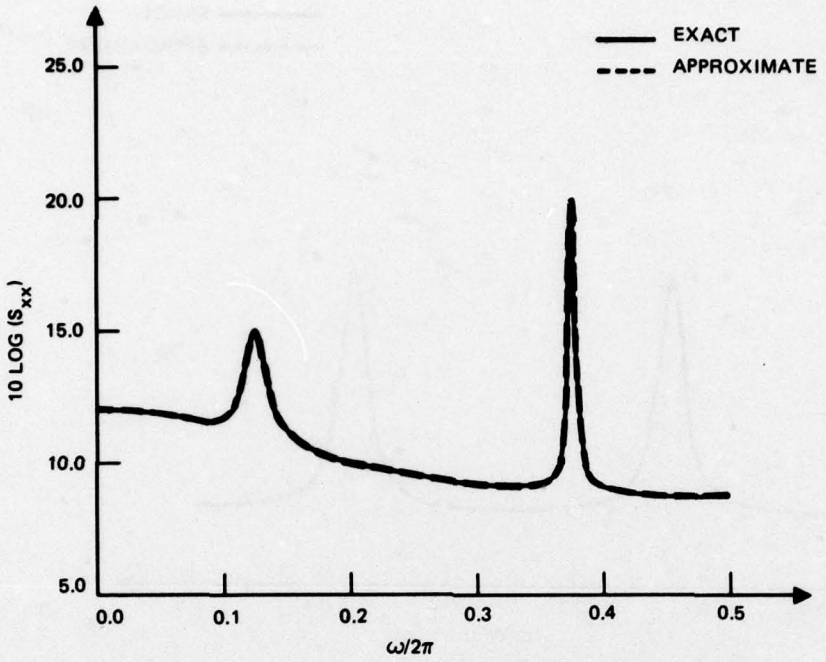

Figure 4. Exact and approximate plots of $S_{xx}(e^{j\omega})$ *(in dB) for* $\sigma_1^2 = \sigma_2^2 = 1.0$; $P_0 = P_1 = 5.0$; $\alpha_0 = 1.0$; $\alpha_1 = 0.05$; $\alpha_2 = 0.01$; $f_1 = 0.125$; and $f_2 = 0.375$.

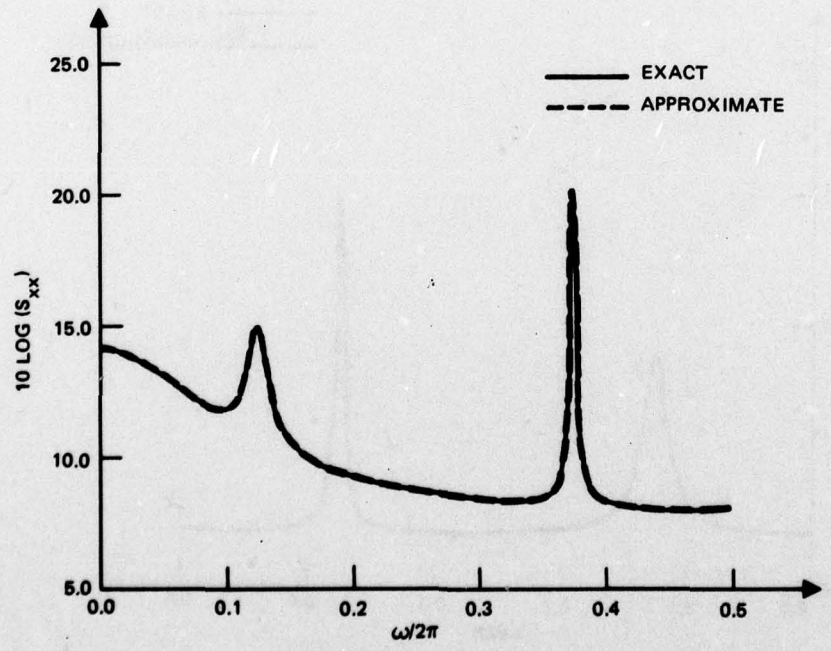

Figure 5. Exact and approximate plots of $S_{xx}(e^{j\omega})$ **(in dB) for** $\sigma_1^2 = \sigma_2^2 = 1.0$; $P_0 = P_1 = 5.0$; $\alpha_0 = 0.50$; $\alpha_1 = 0.05$; $\alpha_2 = 0.01$; $f_1 = 0.125$; and $f_2 = 0.375$.

THE LPF IMPULSE RESPONSE AND TRANSFER FUNCTION

Under the assumption of small α_n so that Eq. (13) is valid, we can now obtain the impulse response, $w^*(k)$ ($k = 0, 1, \ldots, L-1$) directly from Eq. (4). In order to gain some insight into the analytic structure of $w^*(k)$, it is useful to decompose the impulse response as follows:

$$w^*(k) = h_s(k) + h_{no}(k) \qquad k = 0, 1, \ldots, L-1. \tag{16}$$

In Eq. (16) $h_s(k)$ consists solely of damped exponentials at the signal zeroes and is given by:

$$h_s(k) = \sum_{n=1}^{2N} \left\{ B_n^{+s} e^{-\beta_n k + j\omega_n k} + B_n^{-s} e^{-\beta_n (L-1-k) + j\omega_n k} \right\}, \tag{17}$$

where $\omega_{n+N} \equiv -\omega_n$ ($n = 1, 2, \ldots, N$). β_n is given by Eq. (13), and the determination of the $B_n^{\pm s}$ will be discussed presently. Also in Eq. (16), $h_{no}(k)$ is given by:

$$h_{no}(k) = \sum_{m=1}^{M_o} \left\{ B_m^{+0} e^{-\mu'_m k + j\theta'_m k} + B_m^{-0} e^{-\mu'_m (L-1-k) + j\theta'_m k} \right\}$$
$$+ \sum_{r=1}^{N_o - M_o} \left\{ C_r^{+0} \delta(k - r + 1) + C_r^{-0} \delta(k + r - L) \right\}. \tag{18}$$

In Eq. (18), the μ'_m and θ'_m are defined by Eq. (11) and the constants $B_m^{\pm 0}$, $C_r^{\pm 0}$, as well as the $B_n^{\pm s}$ in Eq. (17) are determined as in Eqs. (5) and (6).

As can be seen from Eq. (17), $h_s(k)$ is closely connected with the signal part of the input spectrum and $h_{no}(k)$ is associated with the noise part. However, h_s and h_{no} are coupled together through the constants, $B_n^{\pm s}$, $B_m^{\pm 0}$, and $C_r^{\pm 0}$. In order to further understand this coupling, one must analytically treat Eqs. (5) and (6). Such a treatment, which is straightforward (though tedious), has been carried out in Appendix D and some useful approximate results are obtained for two important limiting cases of practical interest.

Description of LPF for $L \to \infty$

The first limiting case considered is that of large filter length. Specifically, for this case we require that:

$$L \gg \frac{1}{\mu'_m}, \qquad \text{for all } m = 1, 2, \ldots, M_o \tag{19a}$$

and

$$L \gg \frac{1}{\beta_n}, \qquad \text{for all } n = 1, 2, \ldots, 2N. \tag{19b}$$

This particular case provides an indication of the limiting resolution which can be achieved by the LPF. As discussed in Appendix D, when Eq. (19) is satisfied and when the β_n are

very small (narrowband signal case), the B_n^{-s} approach zero and the equations for the B_n^{+s} uncouple (approximately) resulting in the following expressions for the B_n^{+s} (Appendix D, Eq. (D-13)):

$$B_n^{+s} \approx (\beta_n - \alpha_n)\, e^{-\alpha_n \Delta + j\omega_n \Delta} \qquad n = 1, 2, \ldots, 2N, \tag{20}$$

where in Eq. (20), $\alpha_{n+N} \equiv \alpha_n$ and $\omega_{n+N} \equiv -\omega_n$ ($n = 1, 2, \ldots, N$). The approximations required for the validity of Eq. (20) include Eq. (19) plus the conditions:

$$\beta_n - \alpha_n \ll 1 \qquad n = 1, 2, \ldots, N \tag{21a}$$

and

$$1/\alpha'_m \ll \Delta \ll 1/\alpha_n, \qquad \text{for all } n,m. \tag{21b}$$

Note that the noise decorrelation condition Eq. (21b) is consistent with the broadband noise assumption expressed by Eq. (12).

Therefore, from Eqs. (17) and (20), it is seen that for large L, the signal part of the LPF impulse response, $h_s(k)$, will consist of a sum of damped exponentials decaying away from the beginning of the filter and the amplitudes of these exponentials, $\beta_n - \alpha_n$, are all small. Additional insight into the signal part of the LPF may be obtained by examining the frequency response of $h_s(k)$, i.e.,

$$H_\infty^s(\omega) \equiv e^{-j\omega} \sum_{k=0}^{\infty} h_s(k)\, e^{-j\omega k} \approx \sum_{n=1}^{2N} H_n^s(\omega) \tag{22a}$$

where

$$H_n^s(\omega) \equiv e^{-j\omega} \frac{(\beta_n - \alpha_n)\, e^{-\alpha_n \Delta + j\omega_n \Delta}}{1 - (1 - \beta_n)\, e^{j(\omega_n - \omega)}}. \tag{22b}$$

Equation (22) reveals that the signal part of the LPF transfer function for large L consists of sums of decoupled bandpass filters, $H_n^s(\omega)$, centered at the signal frequencies. The gain of the n^{th} filter at its center frequency is given by

$$|H_n^s(\omega_n)| = \left(1 - \frac{\alpha_n}{\beta_n}\right) e^{-\alpha_n \Delta}. \tag{23}$$

For small values of α_n, the value of this gain (from Eq. (14) and provided Eq. (21b) holds) is given approximately by

$$|H_n^s(\omega_n)| \approx 1 - (1 + \mathrm{SNR}_n/\alpha_n)^{-1/2}. \tag{24a}$$

Note from Eq. (24a) that as SNR_n/α_n approaches zero, $|H_n^s(\omega_n)|$ approaches zero as

$$\frac{1}{2}\,\mathrm{SNR}_n/\alpha_n. \tag{24b}$$

Vice versa, as SNR_n/α_n becomes large, $|H_n^s(\omega_n)|$ approaches unity as:

$$1 - (\alpha_n/SNR_n)^{1/2}. \tag{24c}$$

Also, it is seen from Eq. (23) that as $\alpha_n\Delta$ becomes large (so that Eq. (21b) is violated), the signal as well as the noise is decorrelated by the LPF and $|H_n^s(\omega_n)|$ approaches zero.

Another property of the n^{th} decoupled signal filter which is revealed by Eq. (22b) is that its 3-dB half-bandwidth is approximately equal to β_n (in angular frequency). This property along with Eqs. (13) through (15) show that only for small values of SNR_n ($SNR_n < \alpha_n$) can the n^{th} signal filter bandwidth reduce to the bandwidth of the n^{th} signal as $L \to \infty$. For larger values of SNR_n, the passband of $H_n^s(\omega)$ will become increasingly wider than the signal bandwidth. This widening effect has the simple interpretation that when there is little noise in the vicinity of the signal, the LPF frequency response can afford to widen at the signal frequency. This is possible since there is very little input noise power near the signal which will pass through to the LPF output. However, as the input power in the relatively uncorrelated noise increases near the signal frequency, the LPF frequency response becomes narrower and smaller in magnitude (24b) in the vicinity of the signal in order to suppress the increased uncorrelated noise as it passes to the LPF output.

Note that the bandwidth and peak magnitude of the LPF output signal power spectrum will mainly depend on the input signal-to-noise spectral density ratio and the input signal bandwidth. Specifically, as the ratio, SNR/α, becomes small, the gain of the LPF at the center frequency of the signal approaches zero (from Eq. (24b)), and the 3-dB bandwidth of the LPF approaches the 3-dB bandwidth of the signal ((13) - (15)). Therefore, in this limit the peak magnitude of the LPF output signal power spectrum will approach zero and the 6-dB bandwidth of the output signal will approach the 3-dB bandwidth of the input signal, thereby producing considerable distortion in the output signal power spectrum. However, for large values of SNR/α, the gain of the LPF at the center frequency of the signal approaches unity (from Eq. (24c)) and the 3-dB bandwidth of the LPF becomes increasingly larger than that for the signal ((13) - (15)). Therefore, as SNR/α becomes larger, the peak magnitude and 3-dB bandwidth of the output signal power spectrum are approximately equal to that for the input signal power spectrum, thereby producing little signal distortion.

Another term which remains to be discussed is that part of the LPF which is associated with the noise, i.e., $h_{no}(k)$ which is given by Eq. (18). As discussed in Appendix D, when Eq. (19) is satisfied, the C_r^{-0} and B_m^{-0} in Eq. (18) approach zero and $h_{no}(k)$ will only consist of damped exponentials and delta functions which occur at the beginning of the filter. Also, as discussed in Appendix D, when Eq. (21) is satisfied the B_m^{+0} and C_r^{+0} in Eq. (18) can be expressed as linear combinations of the B_n^{+s} which are given approximately by Eq. (20).

Further insight into the noise part of the LPF may be obtained by examining the frequency response of $h_{no}(k)$, i.e.,

$$H_\infty^0(\omega) \equiv e^{-j\omega} \sum_{k=0}^{\infty} h_{no}(k)\, e^{-j\omega k}$$

$$= \sum_{m=1}^{M_o} H_m^0(\omega) + \sum_{r=1}^{N_o-M_o} G_r^0(\omega) \tag{25a}$$

where

$$H_m^0(\omega) = \frac{e^{-j\omega} B_m^{+0}}{1 - e^{-\mu'_m + j(\theta'_m - \omega)}}, \tag{25b}$$

and

$$G_r^0(\omega) = C_r^{+0} e^{-j\omega r}. \tag{25c}$$

Note that the peak magnitude value of the $H_n^0(\omega)$ is given by

$$|H_m^0(\theta'_m)| = \frac{|B_m^{+0}|}{1 - e^{-\mu'_m}}, \tag{26}$$

and the peak magnitude of $G_r^0(\omega)$ is simply

$$|G_r^0(\omega)| = |C_r^{+0}|. \tag{27}$$

The relations expressed by Eqs. (25) through (27) reveal that in general the noise part of the LPF frequency response can contribute non-negligible peaks to the total LPF transfer function, especially if some of the μ'_m are close to zero (as can be seen from Eq. (26)). However, since the B_m^{+0} and C_r^{+0} are linearly related to the B_n^{+s} as discussed previously, the magnitudes B_m^{+0} and C_r^{+0} will become increasingly small as the differences, $\beta_n - \alpha_n$, all approach zero as can be seen from Eq. (20). Therefore, provided the noise spectrum does not contain deep nulls (i.e., small μ'_m) and provided that the $\beta_n - \alpha_n$ are all very small (e.g., narrowband signal case), then the noise part of the LPF frequency response will be very small.

For purposes of numerically examining the approximate expressions derived in this section, plots are presented in Figures 6–8 of $|H_L(\omega)|^2$ computed exactly using Eq. (1) and computed approximately using Eq. (22) for three representative cases. (Note that the approximate expression given by Eq. (22) does not include the noise contributions to the LPF transfer function.) In these figures, the forms of the input signal and noise autocorrelation functions are equivalent to that used in Figures 2–5. Figures 6 and 7 correspond to the case of uncorrelated input noise. As is seen in these two figures, there is excellent agreement between the exact curve and the approximate curve (computed from Eq. (22)). Figure 8 corresponds to the case when the power spectral density of the input noise varies as a function of the frequency. Note that in this figure, there is excellent agreement in the vicinity of the signal peaks. However, there are discrepancies between the exact and approximate curves especially at f = 0. These discrepancies are mainly due to the contributions from the noise part of the LPF which are not included in the computation of the approximate curve. The close agreement between the exact and approximate curves is indicative of the fact that the noise contributions to the LPF transfer function are negligible when Eq. (21b) is satisfied.

It is interesting to compare Figures 6 and 8 with Figures 3 and 5, especially at the signal frequency $f_2 = 0.375$. The increased 3-dB bandwidth of the LPF over the input signal 3-dB bandwidth is clearly seen.

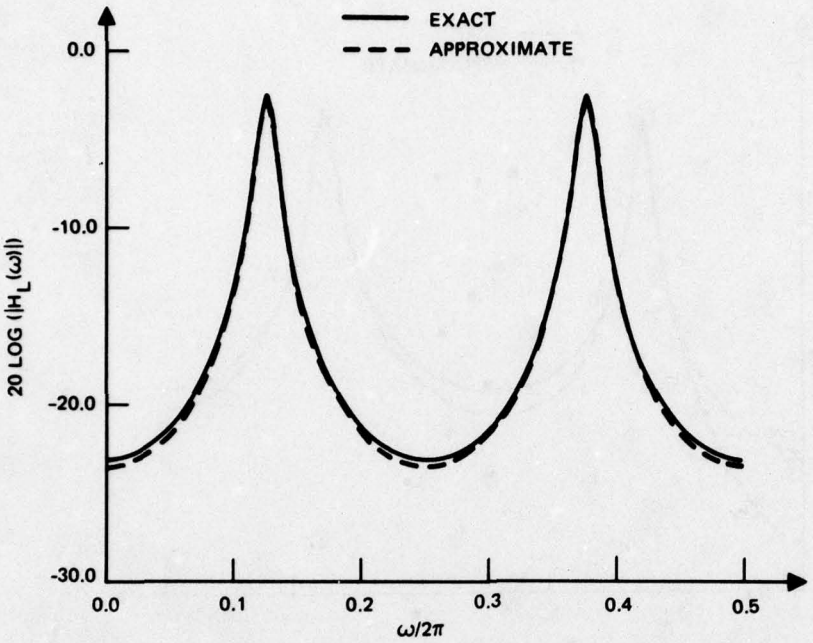

Figure 6. Exact and approximate plots of $|H_L(\omega)|^2$ (in dB) for $\sigma_1^2 = \sigma_2^2 = 1.0$; $P_0 = 5.0$; $P_1 = 0$; $\alpha_1 = \alpha_2 = 0.01$; $f_1 = 0.125$; $f_2 = 0.375$; $L = 256$; and $\Delta = 1$.

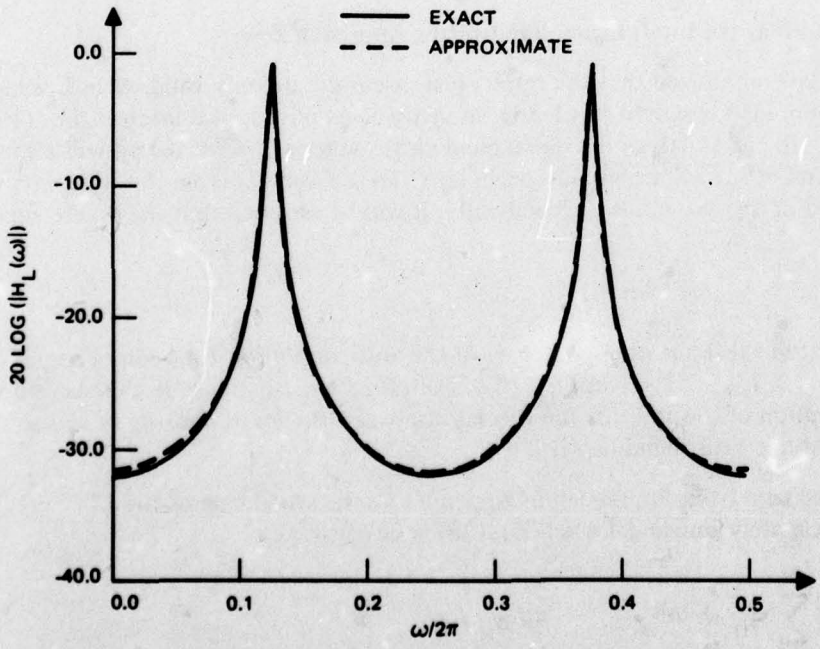

Figure 7. Exact and approximate plots of $|H_L(\omega)|^2$ (in dB) for $\sigma_1^2 = \sigma_2^2 = 1.0$; $P_0 = 5.0$; $P_1 = 0$; $\alpha_1 = \alpha_2 = 0.001$; $f_1 = 0.125$; $f_2 = 0.375$; $L = 256$; and $\Delta = 1$.

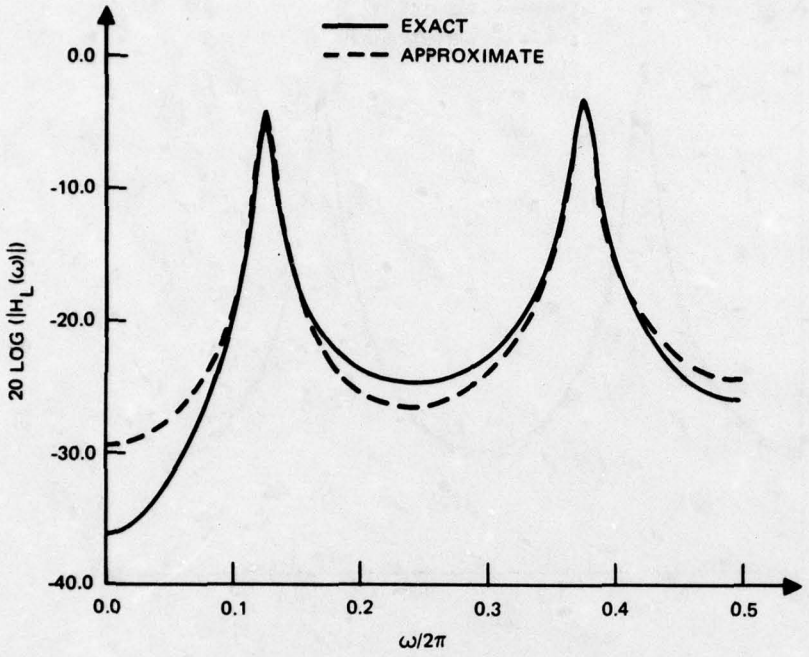

Figure 8. Exact and approximate plots of $|H_L(\omega)|^2$ (in dB) for $\sigma_1^2 = \sigma_2^2 = 1.0$; $P_0 = P_1 = 5.0$; $\alpha_0 = 0.5$; $\alpha_1 = \alpha_2 = 0.01$; $f_1 = 0.125$; $f_2 = 0.375$; $L = 256$; and $\Delta = 10$.

Description of LPF as the Input Signal Bandwidths Approach Zero

It must be emphasized that the results just discussed are only valid when L is large enough so that Eq. (19) is satisfied. Clearly, in many cases of practical interest, Eq. (19) will not be satisfied. In particular, as the signal bandwidths approach zero, the β_n will also approach zero and (19b) will eventually be violated for L fixed. It is this limiting case which will be examined in this subsection. Specifically, it will be assumed that the α_n are small enough so that:

$$L \ll 1/\beta_n, \qquad \text{for all } n = 1, \ldots, 2N. \tag{28}$$

Note that in this limit, the signal part of the autocorrelation function becomes purely sinusoidal for $k = 0, 1, \ldots, L-1$ in Eq. (10). Therefore, the treatment in this section will provide a description of the LPF for the special case when the input consists of sinusoids embedded in additive broadband noise.

As can be seen from Eq. (D-19) in Appendix D, the signal part of the LPF, $h_S(k)$, becomes approximately sinusoidal when Eq. (28) is satisfied, i.e.,

$$h_s(k) \approx \sum_{n=1}^{2N} A_n e^{j\omega_n k}, \qquad \text{for } \alpha_n \approx 0. \tag{29}$$

As discussed in Appendix D, when L is large enough for the LPF to resolve the sinusoids but yet small enough so that Eq. (28) is satisfied, then the A_n are given approximately by (Appendix D, Eq. (D-20)):

$$A_n \approx \frac{SNR_n/2}{1 + LSNR_n/2} e^{j\omega_n \Delta}. \tag{30}$$

The validity of Eq. (30) also requires that the background noise be decorrelated by the LPF, i.e., Eq. (21b) must be satisfied.

Equations (29) through (30) imply that the frequency response of the signal part of the LPF, $H_L^s(\omega)$ can be approximated by a superposition of uncoupled bandpass filters, i.e.,

$$H_L^s(\omega) \approx \sum_{n=1}^{2N} T_n^s(\omega), \tag{31a}$$

where

$$T_n^s(\omega) \equiv \left(\frac{e^{-j\omega}(SNR_n/2)\, e^{j\omega_n \Delta}}{1 + LSNR_n/2}\right)\left(\frac{1 - e^{j(\omega_n - \omega)L}}{1 - e^{j(\omega_n - \omega)}}\right). \tag{31b}$$

The gain of the n^{th} filter at its center frequency is given by:

$$|T_n^s(\omega_n)| = \frac{LSNR_n/2}{1 + LSNR_n/2}. \tag{32}$$

The results expressed by Eqs. (29) through (32) are straightforward extensions of the results presented in References [12] and [22] for the uncorrelated background noise case. A further discussion can be found in these references.

The noise part of the LPF, $h_{no}(k)$ in Eq. (18), may be treated in analogy with the treatment already presented (i.e., Eqs. (25) through (27)). Specifically provided Eq. (21b) is satisfied, the $B_m^{\pm 0}$ and $C_r^{\pm 0}$ in Eq. (18) will be linearly related to the A_n as discussed in Appendix D. Further, when the magnitude of the A_n are small and provided there are no deep nulls in the input noise spectrum (as discussed in the previous subsection), then the effects of the noise part of the LPF will be small.

Plots of $|H_L(\omega)|^2$ which compare the exact solution for $|H_L(\omega)|^2$ obtained from Eq. (1) as well as the approximations provided by Eq. (31) are presented in Figures 9–10 for two representative cases. In these two figures, the forms of the signal and noise autocorrelation functions are equivalent to that used in Figures 2–8. In Figure 9, the input noise is correlated. As in the case of Figure 8, there is good agreement between the exact and approximate curves near the signal peaks, but some discrepancies near f = 0. These discrepancies are mainly the result of ignoring the noise part of the LPF in computing the approximate curve. In Figure 10, the input noise is uncorrelated and the signal bandwidths are chosen such that Eqs. (31) and (22) provide good approximations to the LPF response to the signals at f = 0.125 and f = 0.375, respectively. Therefore, the LPF can be approximated as a sum of two bandpass filters centered at f = 0.125 and f = 0.375, with Eqs. (31) and (22) providing good approximations to the bandpass filters located at f = 0.125 and f = 0.375, respectively.

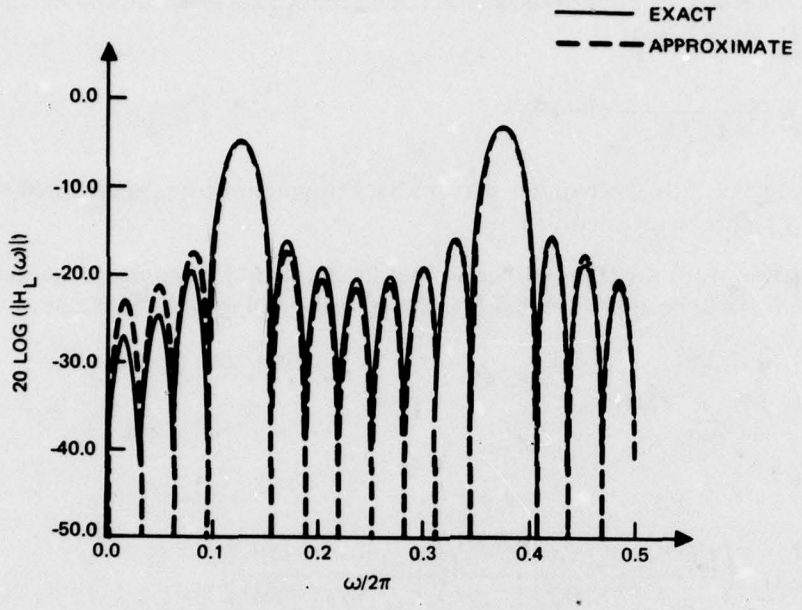

Figure 9. Exact and approximate plots of $|H_L(\omega)|^2$ (in dB) for $\sigma_1^2 = \sigma_2^2 = 1.0$; $P_0 = P_1 = 5.0$; $\alpha_0 = 0.5$; $\alpha_1 = \alpha_2 = 0.001$; $f_1 = 0.125$; $f_2 = 0.375$; $L = 32$; and $\Delta = 10$.

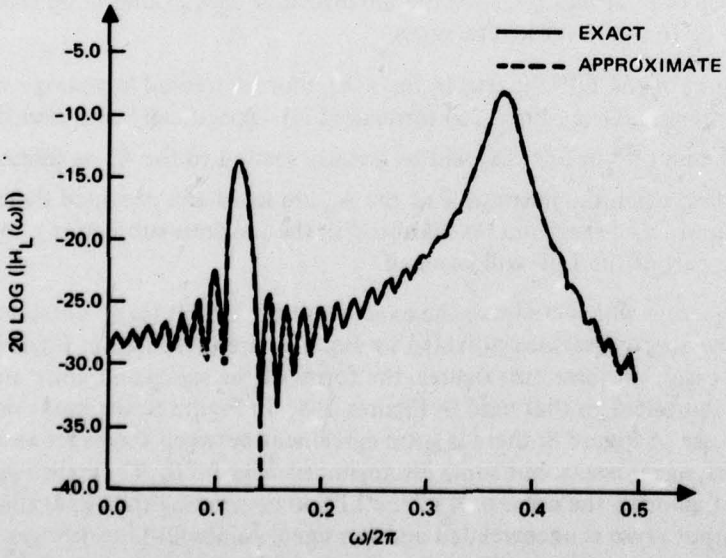

Figure 10. Exact and approximate plots of $|H_L(\omega)|^2$ (in dB) for $\sigma_1^2 = 0.05$; $\sigma_2^2 = 0.5$; $P_0 = 5.0$; $P_1 = 0$; $\alpha_1 = 0.001$; $\alpha_2 = 0.05$; $f_1 = 0.125$; $f_2 = 0.375$; $L = 64$; $\Delta = 1$.

As is seen in Figure 10, this approximation provides good agreement with the exact curve. Note that the behavior of the LPF in the vicinity of f = 0.125 is oscillatory in contrast to its behavior at f = 0.375. This is a consequence of the fact that the LPF has completely resolved ($\beta_L > 1$), the signal at f = 0.375.

The approximate expressions given by Eq. (22) for large values of $L\beta_n$ and those given by Eq. (31) for small values of $L\beta_n$ will provide a good description of an LPF for a rather broad class of inputs which consist of narrowband processes and additive noise. Specifically, for an input consisting of N narrowband signals in noise, the LPF will form bandpass filters at the signal frequencies (provided the components of $h_S(k)$ in Eq. (17) decouple). The analytical structure of the n^{th} bandpass filter will then be described either by Eq. (22) or Eq. (31) depending on whether $L\beta_n \gg 1$ or $L\beta_n \ll 1$, respectively (as in Figure 10). When $L\beta_n \approx 1$, then $h_S(k)$ will consist of damped exponentials decaying away from both ends of the filter (see Eq. (17)). Assuming the components of $h_S(k)$ decouple, then an approximate expression for the n^{th} bandpass filter when $L\beta_n \approx 1$ may be obtained by solving the two simultaneous equations for B_n^{+s} and B_n^{-s} which are provided by Eqs. (5) and (6) (with all the $C_r^{\pm} = 0$ and N = M = 1 in Eqs. (5) and (6)).

A DERIVATION OF THE LPF FOR AN ALL-POLE NOISE SPECTRUM

In the last subsection, properties of the LPF were discussed for inputs consisting of signals and noise. In this section, we will examine the special case when all of the signal powers vanish and when the noise spectrum contains only poles. This particular case is of interest as it provides additional insight into the basic structure of the LPF. For this special case, $S_{xx}(z)$ has the form:

$$S_{xx}(z) = \frac{\sigma_o^2}{\prod_{n=1}^{p} (z - z_n)(z^{-1} - \bar{z}_n)}, \tag{33}$$

where σ_o^2 is a real positive constant and all the z_n in Eq. (33) are assumed to lie inside the unit circle.

The spectral representation in Eq. (33) is equivalent to the time series model representation for x(j) [17]:

$$x(j) = \sum_{k=0}^{p-1} a_k x(j - k - 1) + u(j), \tag{34}$$

where u(j) is an uncorrelated sequence with power equal to σ_o^2. A process which can be represented as in Eq. (34) is termed an autoregressive (AR) process of order p. From Eq. (33) it is seen that a FIR filter of order p can produce an output with a completely flat spectrum when the input to the filter is an AR or all-pole process. In fact, from Eq. (34), it is seen that the required coefficients for a FIR "whitening" filter are given by:

$$\{1, -a_0, -a_1, \ldots, -a_{p-1}\}. \tag{35}$$

This fact, together with the "whitening" filter interpretation of the LPF discussed in Section II reveals that provided $\Delta = 1$ in Figure 1, the LPF coefficients, $w^*(k)$, of an L-point prediction filter ($L \geq p$) will be given by

$$w^*(k) = \begin{cases} a_k, k = 0, 1, \ldots, p-1 \\ 0, k = p, \ldots, L \end{cases} . \tag{36}$$

The connection between the a_n in Eq. (34) and the coefficients of a p-point LPF can be derived alternatively by multiplying both sides of Eq. (34) by $x(j - \ell - 1)$ and taking expectations. The resulting equations for $\ell = 0, 1, \ldots, p-1$ are given by

$$\sum_{k=0}^{p-1} a_k \phi_{xx}(\ell - k) = \phi_{xx}(\ell + 1) \qquad \ell = 0, 1, \ldots, p-1, \tag{37}$$

which are identical to Eq. (1) for the LPF coefficients, $w^*(k)$, with $L = p$. Another property of the a_k which relates them to the z_n in Eq. (33), is given by Eqs. (5) and (6) (with $\Delta = 1$; $N = p$; $C_k^+ = a_{k-1}$; $z_n = e^{-\alpha_n + j\omega_n}$; and $B_m^{\pm}$, $C_r^- \approx 0$), i.e.,

$$\sum_{k=0}^{p-1} a_k z_n^{-k} = z_n \qquad n = 1, \ldots, p. \tag{38}$$

It should be noted that Eq. (38) is equivalent to the relationship between the a_k and z_n which is derived by equating powers of z^{-n} between the polynomial

$$1 - \sum_{k=0}^{p-1} a_k z^{-k-1}, \tag{39a}$$

and the expansion

$$\prod_{n=1}^{p} (1 - z^{-1} z_n). \tag{39b}$$

The $p \times p$ coefficient matrix of the a_k in Eq. (38) is a Vandermonde matrix and many of its properties were derived in Reference [25] for purposes of treating the continuous analog of Eq. (1). (See also References [26] and [27].) In the general case when $\Delta > 1$ and $S_{xx}(z)$ is given by Eq. (33), there will still be only p non-zero LPF coefficients for an L-point prediction filter ($L \geq p$), however, these coefficients will satisfy (from Eqs. (5) and (6)):

$$\sum_{k=0}^{p-1} w^*(k) z_n^{-k} = z_n^{\Delta} \qquad n = 1, 2, \ldots, p. \tag{40}$$

An alternative treatment of the all-pole noise case for $\Delta > 1$ is given in Reference [28], Chapter 7.

IV. HARDWARE SIMULATIONS OF AN ADAPTIVE IMPLEMENTATION OF AN LPF

As discussed in Section I, there are many adaptive implementations of Wiener filters which continuously estimate the Wiener filter coefficients. In this section, we will examine the steady state response of an LMS adaptive filter [3-5] to three types of stationary inputs– one-pole low pass noise, a narrowband signal plus one-pole low pass noise, and a sinusoid in bandlimited noise. As will be seen, the analysis presented in Sections II and III will provide a good description of the experimental results presented in this section.

The specific configuration of the LMS adaptive filter considered in this section is known as the Adaptive Line Enhancer (ALE). The LMS algorithm for the ALE is as follows:

$$w_{j+1}(k) = w_j(k) + 2\mu x(j - \Delta - k)\, e(j) \tag{41a}$$

and,

$$e(j) = x(j) - \sum_{n=0}^{L-1} x(j - \Delta - n)\, w_j(n), \qquad k = 0, 1, \ldots, L - 1. \tag{41b}$$

In Eq. (41), $w_j(k)$ represents the k^{th} ALE filter coefficient at iteration j; μ is a scalar representing the influence of the input x(j) on the (j + 1) update of w(k); and L and Δ are, respectively, the number of weights and the delay.

A summary of many of the properties of the ALE can be found in References [12], [21], [29], and [35]. As discussed in these references, provided μ is small enough and provided the input data is statistically stationary, then the mean of the ALE filter weights will converge within a good approximation to the LPF coefficients described by Eq. (1). Since the effective integration time of the ALE is finite, the steady-state ALE filter coefficients will contain a random fluctuating component. However, the variance of this component can be kept arbitrarily small by reducing $\mu\, \phi_{xx}(0)$ (at the expense of increasing the ALE convergence time). In the experiments described in this section, μ was kept small enough that weight vector noise was negligible and, therefore, Eq. (1) and the results presented in Sections II and III provided a good description of the steady state response of the ALE.

The experimental data presented in this section were obtained on a variable length hardware implementation of the ALE which was designed and built at the Naval Ocean Systems Center. Filter lengths of 8, 16, 32, 64, 128, and 256 weights can be obtained with this hardware. Experimental plots of the steady state ALE weights were obtained by "freezing" the weights at a particular instant (after convergence). Experimental plots of the steady state frequency response of the ALE were obtained by first "freezing" the weights (after convergence) and then applying white noise to the input of the stationary filter and spectral-analyzing the resulting output. The first case examined was when the ALE input consisted of stationary noise which was generated by passing white noise through a one-pole, low pass filter. For this case, the LPF impulse response consists of only one weight at the beginning of the filter as discussed in the third subsection of Section III, i.e.,

$$w^*(k) = e^{-\alpha\Delta}\delta(k). \tag{42}$$

This was indeed observed as indicated in the experimental plots presented in Figure 11 for three different values of ALE delay, Δ. In this figure, the vertical scale is not absolute,

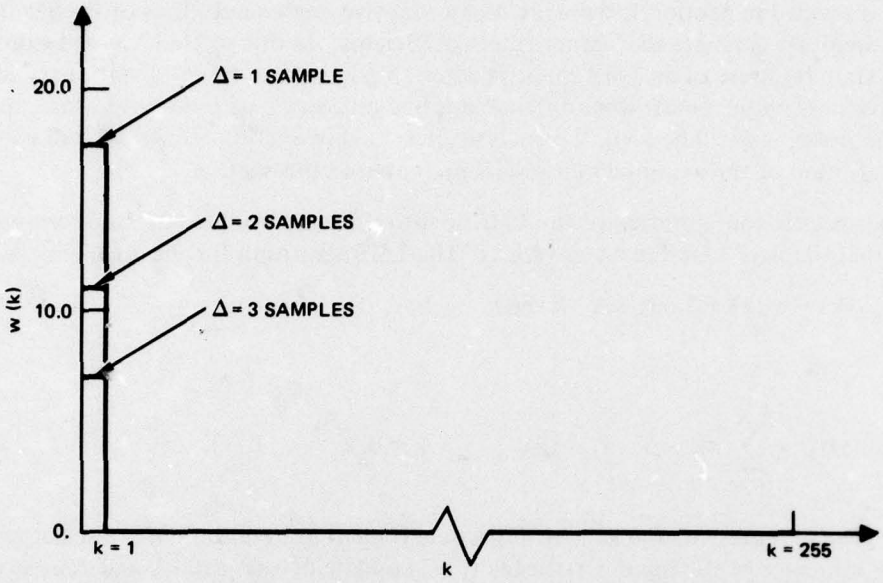

Figure 11. Plot of the ALE weights, w(k), vs k (after convergence) for three different values of delay. The input autocorrelation function, $\phi_{xx}(k)$, was given by $P_0 e^{-\alpha_0 |k|}$ where $\alpha_0 f_s/2\pi$ = 250 Hz and L = 256. The sample frequency, f_s, was 3500 Hz. (P_0 was held constant in all three experiments.)

however, the magnitude of the first weight decreases as exp ($-\alpha\Delta$) with increasing Δ as would be expected from Eq. (42). In fact, the ratio of the measured values of the first weight in Figure 11 is given approximately by: 17.5:11.0:7.0 ≈ 2.5:1.6:1. This compares quite favorably with the theoretical expression for this ratio (Eq. (42)), i.e.,

$$e^{2\alpha\Delta}:e^{\alpha\Delta}:1. \tag{43}$$

Using the measured value for α from Figure 11, it is seen that Eq. (43) predicts the ratio of the first weights to be:

$$e^{4\pi\cdot 250/3500}:e^{2\pi\cdot 250/3500}:1 \approx 2.5:1.6:1,$$

which agrees with the experimental results.

The second experimental case examined corresponds to an input consisting of a narrowband signal embedded in additive one-pole low pass noise. The signal was generated by filtering uncorrelated noise with a two-pole bandpass filter. The bandwidth of the signal was small enough that the sinusoidal approximation is valid. This case illustrates the noise decorrelation property of a variable delay (prediction distance) LPF. The expression for the LPF impulse response may be obtained in Appendix D from Eqs. (D-1), (D-3), (D-16) through (D-18), and (D-19) (with N = 1, N_0 = 1, and M_0 = 0):

$$w^*(k) = A_1 e^{j\omega_1 k} + A_2 e^{-j\omega_1 k} + C_1^{+0}\,\delta(k - r + 1) + C_1^{-0}\,\delta(k + r - L). \tag{44}$$

As can be seen from Eq. (44), the LPF impulse response consists of a sinusoid at the signal frequency as well as two delta functions which occur at the beginning and end of the filter. The constants A_1, A_2, and $C_1^{\pm 0}$ in Eq. (44) can be obtained from Eqs. (D-16) through (D-18). The result is:

$$A_1 = \bar{A}_2 = \frac{e^{j\omega_1 \Delta} - e^{-\alpha\Delta}}{L + 2/SNR + (\cos\omega_1 - e^{-\alpha})/(\cosh\alpha - \cos\omega_1)} \tag{45a}$$

$$C_1^{+0} = e^{-\alpha\Delta} - \sum_{n=1}^{2} \frac{A_n}{1 - e^{-\alpha + j\omega_n}} \tag{45b}$$

$$C_1^{-0} = - \sum_{n=1}^{2} \frac{A_n e^{j\omega_n L}}{1 - e^{-\alpha + j\omega_n}} \tag{45c}$$

and

$$SNR = (\sigma_1^2/P_0) \frac{\cosh\alpha - \cos\omega_1}{\sinh\alpha}, \tag{45d}$$

where in Eq. (45) $\omega_2 = -\omega_1$, and σ_1^2 and P_0 represent the signal power and noise power, respectively. Equation (45a) is only an approximation for A_1. In deriving this approximation, we have neglected all coupling between A_1 and A_2 which occurs in Eqs. (D-16) through (D-18). This approximation is very good in the experimental case we are presently considering. Note that as $\alpha\Delta \to \infty$, and further as $L \to \infty$ and/or $SNR \to 0$, Eq. (45a) reduces to Eq. (30), as expected. Note also that in the limit of large L and/or small SNR, A_1 becomes very small and provided $\alpha\Delta \lesssim 1$, then C_1^{+0} is given approximately by:

$$C_1^{+0} \approx e^{-\alpha\Delta}. \tag{46}$$

The characteristics of the LPF expressed by Eq. (45) were observed as indicated in the experimental plots presented in Figure 12 for two different values of ALE delay, Δ. As in the case of Figure 11, the vertical scale in Figure 12 is not absolute. Also, the sinusoids in Figure 12 were plotted with the frequency, phases, and amplitudes of these sinusoids being estimated from the display of the weights on an oscilloscope. As can be seen, the magnitude of the large impulse at the beginning of the filter decreases as the delay is increased. In fact, the ratio of the measured values of the first weight in Figure 12 is given approximately by: 20.0:6.0 = 3.3:1. Assuming the first weight to be given approximately by Eq. (46) gives the following predicted value for this ratio:

$$e^{6\pi \cdot 250/3500}:1 = 3.9:1.$$

This value is somewhat higher than the measured value. This discrepancy is due, in part, to the fact that we are approximating the first weight by Eq. (46). Another characteristic of the LPF which can be observed in Figure 12 is the increase in the amplitude of the sinusoid in the ALE weights as the delay is increased. The ratio of the measured values of this amplitude in Figure 12 is given by: 0.5:1. The predicted value for this ratio (calculated from Eq. (45a) with $\Delta = 1$ and $\Delta = 4$) is also given by 0.5:1.

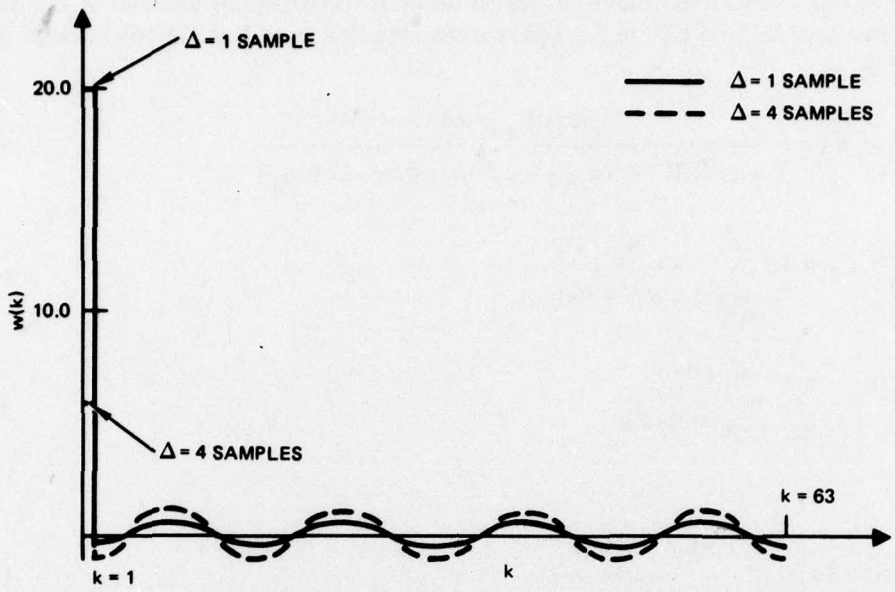

Figure 12. Plot of the ALE weights, w(k), vs k (after covergence) for two different values of delay. The input autocorrelation function, $\phi_{xx}(k)$, was given by $P_0 e^{-\alpha_0|k|} + \sigma_1^2 e^{-\alpha_1|k|} \cos \omega_1 k$ where $\alpha_0 f_s/2\pi = 250$ Hz; $\alpha_1 f_s/2\pi = 0.5$ Hz; $\omega_1 f_s/2\pi = 250$ Hz; and L = 64. The sample frequency, f_s, was 3500 Hz. (P_0/σ_1^2 was held constant in both experiments.)

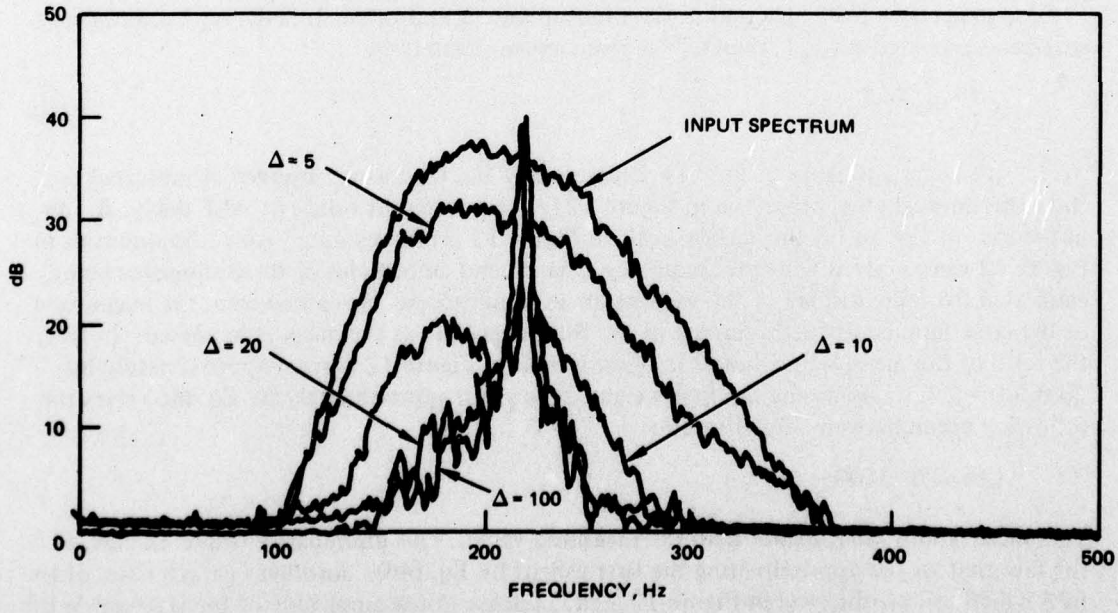

Figure 13. Plots of the steady state ALE frequency response corresponding to four different values of delay for an input consisting of a sinusoid embedded in additive bandlimited noise. The 3-dB bandwidth of the noise was 60 Hz and the sample frequency was 900 Hz. Also, L = 256 and $\mu\, \phi_{xx}(0) = 1.2 \times 10^{-6}$.

The noise decorrelation property of the LPF for this experimental case becomes apparent by noting that the large impulse at the beginning of the filter gives rise to an all pass component in the filter's frequency response. For small values of Δ, the LPF will pass a considerable amount of noise due to this all pass component. However, as Δ is increased, the LPF will suppress more noise as the magnitude of the all pass component decreases. Another example which illustrates the noise suppression capabilities that can be achieved by varying the prediction distance of the LPF is presented in Figure 13. In this figure, the steady state frequency response of the ALE is plotted for four different values of delay when the input consists of a sinusoid embedded in additive bandlimited noise. The noise was generated by filtering white noise through an eight-pole Butterworth low-pass filter followed by an eight-pole Butterworth high pass filter. For purposes of comparison, the input spectrum is also plotted in Figure 13. As indicated in Figure 13, the bandlimited noise is suppressed as Δ is increased but the sinusoid is not attenuated for any value of Δ selected. A similar example was examined in Reference [39]. Additional experiments which compare the steady state LMS filter response with a theoretical Wiener filter may be found in References [12], [29], and [36].

V. CONCLUSIONS

In this report the Impulse Response (IR) and Frequency Response (FR) of a discrete LPF were examined for stationary inputs consisting of narrowband signals embedded in broadband additive noise. In Section II the general analytic form of the IR and FR were derived for the general case when the z-transform, $S_{XX}(z)$, of the autocorrelation function of the input was a rational function of z. It was shown that the IR consists of sums of damped exponentials and impulses which occur at both ends of the LPF. Further, the amplitudes of the exponentials and impulses which occur at the end of the LPF (reflection amplitudes) approach zero as the length of the LPF becomes large.

In Section III, inputs consisting of narrowband signals and additive noise, were examined in detail. Specifically, in the first major subsection of Section III, rational spectrum models were developed to approximate the true input power spectrum of the signals and noise. In the next area of Section III, the results of Section II were used to examine the IR and FR of the LPF for two limiting cases. First, when the length of the LPF becomes very large, it was shown that its FR can be approximated by a superposition of decoupled bandpass filters located at the signal frequencies. The gain of these filters at their center frequencies were shown to approach unity as the product of the input signal-to-noise spectral density ratio and the inverse signal 3-dB half bandwidth, i.e., SNR/α, becomes large. Also, the bandwidths of these decoupled filters were shown to become increasingly wider than the signal bandwidths as the ratios, SNR/α, become large. Therefore, only for large values of SNR/α can the LPF filter the input noise without distorting the signal in the limit of large filter lengths.

A second limiting case was considered when all of the signal bandwidths approach zero (sinusoidal limit). In this limit, it was shown that the LPF also forms a superposition of bandpass filters located at the signal frequencies. As the product, L SNR/2, becomes large it was shown that the gain of these filters approaches unity. Therefore, only for large values of L SNR/2 can the LPF filter the input noise without distorting the peak magnitude of the output signal power spectrum in the sinusoidal limit. The special case when the LPF input consists solely of all-pole noise was treated next a[illegible]ly, in Section IV, results of an

experimental simulation of an adaptive implementation of an LPF were presented and discussed. It was shown that appropriate selection of the prediction distance Δ can provide an enhancement of the narrowband signal components by suppressing the additive broadband noise contributions to the LPF impulse response.

APPENDIX A. GENERAL FORM OF THE DISCRETE LPF FOR STATIONARY INPUTS WITH RATIONAL POWER SPECTRUM REPRESENTATIONS

The purpose of this appendix is to develop a general form for the solution, $w^*(k)$ $(k = 0, \ldots, L-1)$, to the discrete analog of the Wiener-Hopf equation:

$$\sum_{k=0}^{L-1} w^*(k)\, \phi_{xx}(\ell-k) = \phi_{xx}(\ell+\Delta) , \qquad \ell = 0, \ldots, L-1 , \tag{A-1}$$

when the z-transform of $\phi_{xx}(k)$, $S_{xx}(z)$, is a rational function of z. The specific form of $S_{xx}(z)$ considered here is

$$S_{xx}(z) = A \frac{\prod_{m=1}^{M} \left(z - e^{-\mu_m + j\theta_m}\right)\left(z^{-1} - e^{-\mu_m - j\theta_m}\right)}{\prod_{n=1}^{N} \left(z - e^{-\alpha_n + j\omega_n}\right)\left(z^{-1} - e^{-\alpha_n - j\omega_n}\right)} , \tag{A-2}$$

where the μ_m and α_n are non-zero, positive real constants and

$$-\pi \leq \omega_n, \theta_m \leq \pi , \text{ for all m,n,}$$

and A is a real, positive constant.

The treatment of Eq. (A-1) presented in this appendix represents a brief summary of the rigorous treatments given in References [14] and [16] for the discrete problem and is analogous to the treatments given in References [19], [25], and [31] for the continuous problem. Alternative treatments of Eq. (A-1) or its continuous analog include the interesting development given in Reference [30] (Appendix E). To develop a simple expression for $w^*(k)$, we first note that if the power spectrum of x can be represented by Eq. (A-2) with $z = \exp(j\omega)$, then x(j) must obey a difference equation given by:

$$D(z^{-1})\, x(j) = P(z^{-1})\, u(j) . \tag{A-3}$$

In Eq. (A-3), $D(z^{-1})$ and $P(z^{-1})$ denote linear difference operators and u(j) represents a stationary, uncorrelated sequence with power given by A in Eq. (A-2), i.e.,

$$E[u(j)\, u(j+m)] = A\delta(m) . \tag{A-4}$$

The specific forms of D and P are given by:

$$D(z^{-1}) = \prod_{n=1}^{N} (1 - e^{-\alpha_n + j\omega_n} z^{-1})$$

$$= \sum_{n=0}^{N} a_n z^{-n} \tag{A-5a}$$

and,

$$P(z^{-1}) = \prod_{m=1}^{M} \left(1 - e^{-\mu_m + j\theta_m} z^{-1}\right)$$

$$= \sum_{m=0}^{M} b_m z^{-m} , \qquad \text{(A-5b)}$$

where in Eq. (A-5) $a_o \equiv b_o \equiv 1$. The operation of $D(z^{-1})$ on x(j) in Eq. (A-3) results in a summation of the present and weighted past-values of x(j), i.e.,

$$D(z^{-1})\, x(j) = \sum_{n=0}^{N} a_n\, x(j-n) . \qquad \text{(A-6a)}$$

Similarly, we have for $P(z^{-1})\, u(j)$:

$$P(z^{-1})\, u(j) = \sum_{m=0}^{M} b_m\, u(j-m) . \qquad \text{(A-6b)}$$

We now observe that $\phi_{xx}(\ell-k)$ satisfies Reference [16] (chapter 6):

$$\phi_{xx}(\ell-k) = A\, P_\ell(z^{-1})\, \overline{P_\ell(z)}\, G(\ell-k) , \qquad \text{(A-7a)}$$

where $G(\ell - k)$ (which is a Green's function [16,25]) is obtained from:

$$\overline{D_\ell(z)}\, D_\ell(z^{-1})\, G(\ell-k) = \delta(\ell-k) . \qquad \text{(A-7b)}$$

The conjugate linear operator $\overline{P(z)}$ is defined by

$$\overline{P(z)}\, \phi(j) = \sum_{m=0}^{M} \overline{b_m}\, \phi(j+m) . \qquad \text{(A-8)}$$

A similar definition holds for $\overline{D(z)}$. The "ℓ" subscripts on the operators in Eq. (A-7) denote that they only operate with respect to the ℓ variable in Eq. (A-7). Equation (A-7) may be verified by taking its z-transform (with k=0) and comparing with Eq. (A-2).

Substituting Eq. (A-7a) into Eq. (A-1) results in:

$$\sum_{k=0}^{L-1} w^*(k)\, P_\ell(z^{-1})\, \overline{P_\ell(z)}\, G(\ell - k) = A^{-1}\, \phi_{xx}(\ell + \Delta) \qquad \ell = 0, \ldots, L-1 ,$$

or, by the linearity of the operators:

$$P_\ell(z^{-1})\, \overline{P_\ell(z)}\, F^*(\ell) = A^{-1}\, \phi_{xx}(\ell + \Delta) \qquad \ell = 0, \ldots, L-1 , \qquad \text{(A-9)}$$

where

$$F^*(\ell) \equiv \sum_{k=0}^{L-1} w^*(k)\, G(\ell-k) \ . \tag{A-10}$$

Note that Eq. (A-9) is in the form of an ordinary difference equation with constant coefficients. Therefore, a general solution of Eq. (A-9) is given by Reference [16]:

$$F^*(\ell) = F_h(\ell) + F_p(\ell) \ , \ 0 \leq \ell \leq L-1 \ . \tag{A-11}$$

In Eq. (A-11), $F_h(\ell)$ represents the general solution of the homogeneous equation

$$P_\ell(z^{-1})\, \overline{P_\ell(z)}\, F_h(\ell) = 0 \ , \tag{A-12}$$

and $F_p(\ell)$ represents the particular solution of Eq. (A-9). The general solution of Eq. (A-12), $F_h(\ell)$, can be expressed as a linear superposition of damped exponentials, i.e.,

$$F_h(\ell) = \sum_{m=1}^{M} \left\{ d_m^+ \, e^{-\mu_m \ell + j\theta_m \ell} + d_m^- \, e^{\mu_m \ell + j\theta_m \ell} \right\} \ . \tag{A-13}$$

Note that the exponentials, $z_m \equiv \exp(\pm\, \mu_m + j\theta_m)$, are the roots of the polynomial $P_\ell(z^{-1})\, \overline{P_\ell(z)}$. The particular solution of Eq. (A-9), $F_p(\ell)$, can be obtained by applying to both sides the difference operator, $(P_\ell(z^{-1})\, \overline{P_\ell(z)})^{-1}$, which is inverse to the difference operator, $P_\ell(z^{-1})\, \overline{P_\ell(z)}$. The result for $F_p(\ell)$ is given by Reference [16]:

$$F_p(\ell) = A^{-1} \left(P_\ell(z^{-1})\, \overline{P_\ell(z)} \right)^{-1} \phi_{xx}(\ell + \Delta) \ . \tag{A-14}$$

The final form for $w^*(k)$ can be obtained by applying the operator,

$$\overline{D_\ell(z)}\, D_\ell(z^{-1})$$

to each side of Eq. (A-11) and using Eqs. (A-10) and (A-7b). The resulting expression for $w^*(\ell)$ is given by

$$w^*(\ell) = \overline{D_\ell(z)}\, D_\ell(z^{-1})\, F^*(\ell) \qquad 0 \leq \ell \leq L-1 \ , \tag{A-15a}$$

where

$$F^*(\ell) = \sum_{m=1}^{M} \left\{ d_m^+ \, e^{-\mu_m \ell + j\theta_m \ell} + d_m^- \, e^{\mu_m \ell + j\theta_m \ell} \right\}$$

$$+ A^{-1} \left(P_\ell(z^{-1})\, \overline{P_\ell(z)} \right)^{-1} \phi_{xx}(\ell + \Delta) \qquad 0 \leq \ell \leq L-1 \ . \tag{A-15b}$$

The expression for $w^*(\ell)$ which is obtained from Eq. (A-15) will contain the delta function and its differences at the end points of the interval $0 \leq \ell \leq L-1$. The delta functions arise as a result of applying the operator $\overline{D_\ell(z)}\, D_\ell(z^{-1})$ to $F^*(\ell)$ at the end points $\ell = 0$ and $\ell = L-1$.

Excluding these end point contributions, we have†

$$\overline{D_\ell(z)}\, D_\ell(z^{-1})\, d_m^+ e^{-\mu_m \ell + j\theta_m \ell} = B_m^+ e^{-\mu_m \ell + j\theta_m \ell} \qquad \text{(A-16)}$$

$$0 \leq \ell \leq L-1 \ ,$$

$$\overline{D_\ell(z)}\, D_\ell(z^{-1})\, d_m^- e^{\mu_m \ell + j\theta_m \ell} = B_m^- e^{-\mu_m (L-1-\ell) + j\theta_m \ell}$$

$$0 \leq \ell \leq L-1 \ , \qquad \text{(A-17)}$$

and

$$A^{-1}\, \overline{D_\ell(z)}\, D_\ell(z^{-1}) \left(P_\ell(z^{-1})\, \overline{P_\ell(z)} \right)^{-1} \phi_{xx}(\ell + \Delta) = 0 \ ,$$

$$0 \leq \ell \leq L-1 \ . \qquad \text{(A-18)}$$

Equation (A-18) may be verified by operating on both sides of Eq. (A-7a) with the operator,

$$A^{-1}\, \overline{D_\ell(z)}\, D_\ell(z^{-1}) \left(P_\ell(z^{-1})\, \overline{P_\ell(z)} \right)^{-1} \ ,$$

and using Eq. (A-7b) (with $k = -\Delta$).

Using Eqs. (A-15) through (A-18) and including the delta function contributions at the ends of the interval $0 \leq k \leq L-1$ (as discussed above), we can write the final expression for $w^*(k)$ as (See References [16], chapter 6; and [14], chapter 13.)

$$w^*(k) = \sum_{m=1}^{M} \left\{ B_m^+ e^{-\mu_m k + j\theta_m k} + B_m^- e^{-\mu_m (L-1-k) + j\theta_m k} \right\}$$

$$+ \sum_{r=1}^{N-M} \left\{ C_r^+ \delta(k-r+1) + C_r^- \delta(k+r-L) \right\} \qquad k = 0, \ldots, L-1 \ . \qquad \text{(A-19)}$$

By definition, the sums of the delta functions in Eq. (A-19) vanish when $N \leq M$. When $N > M$, note that N-M delta functions arise at either end of the filter, $w^*(k)$. As shown in Appendix B, this will lead to precisely 2N equations which the 2N constants, $B_m^{\pm}$ and $C_r^{\pm}$, must satisfy.

---

†In operating on the functions on the left hand sides of Eqs. (A-16) through (A-18) with $\overline{D_\ell(z)}\, D_\ell(z^{-1})$, it is tacitly assumed that these functions are extended outside the interval $0 \leq \ell \leq L-1$, i.e., we are ignoring the end point contributions.

APPENDIX B. DERIVATION OF THE COEFFICIENT EQUATIONS FOR THE $B_m^{\pm}$ AND $C_r^{\pm}$

In order to determine the constants $B_m^{\pm}$, $C_r^{\pm}$ which appear in the expansion for $w^*(k)$, one substitutes Eq. (A-19) into Eq. (A-1). Before doing this, however, one must first develop an explicit form for the autocorrelation function, $\phi_{xx}(k)$, from the relation:

$$\phi_{xx}(k) = \frac{1}{2\pi j} \oint_{|z|=1} S_{xx}(z)\, z^{k-1}\, dz \qquad k = 0, \pm 1, \pm 2, \ldots, \tag{B-1}$$

with $S_{xx}(z)$ given by Eq. (A-2). As can be seen from Eq. (A-2), $S_{xx}(z)$ is a rational function of z with poles inside and outside the unit circle. Therefore, Eq. (B-1) can be simply evaluated as the sum of the various pole contributions of $z^{k-1}\, S_{xx}(z)$ which are inside the unit circle, i.e.,

$$\phi_{xx}(k) = \sum_{n=1}^{N} A_n\, e^{-\alpha_n |k| + j\omega_n k} \qquad \text{for} \qquad k \geq 0\ , \tag{B-2a}$$

and

$$\phi_{xx}(k) = \sum_{n=1}^{N} \bar{A}_n\, e^{-\alpha_n |k| + j\omega_n k} \qquad \text{for} \qquad k < 0\ . \tag{B-2b}$$

In Eq. (B-2), A_n is given by:

$$A_n = \frac{B\, e^{(-\alpha_n + j\omega_n)(N-M-1)}}{e^{-\alpha_n + j\omega_n} - e^{\alpha_n + j\omega_n}} \cdot \frac{\prod_{m=1}^{M} \left(e^{-\alpha_n + j\omega_n} - e^{-\mu_m + j\theta_m}\right)\left(e^{-\alpha_n + j\omega_n} - e^{\mu_m + j\theta_m}\right)}{\prod_{\substack{\ell=1 \\ \ell \neq n}}^{N} \left(e^{-\alpha_n + j\omega_n} - e^{-\alpha_\ell + j\omega_\ell}\right)\left(e^{-\alpha_n + j\omega_n} - e^{\alpha_\ell + j\omega_\ell}\right)}, \tag{B-3a}$$

where B is given by

$$B = (-1)^{M-N} \left[\prod_{m=1}^{M} e^{-\mu_m - j\theta_m} \Big/ \prod_{n=1}^{N} e^{-\alpha_n - j\omega_n} \right] A\ , \tag{B-3b}$$

and A is defined by Eq. (A-2). In deriving the expansion for $\phi_{xx}(k)$ given by Eq. (B-2), it has been tacitly assumed that $M < N$. When $M \geq N$ then Eq. (B-2) must be modified to include a linear combination of the delta functions: $\delta(k), \delta(k \pm 1), \ldots, \delta(k \pm (M-N))$.

Substituting Eq. (A-19) for $w^*(k)$ into Eq. (A-1) with $\phi_{xx}(k)$ given by Eq. (B-2) leads to the following equation:

$$\sum_{m=1}^{M}\sum_{n=1}^{N}\left\{B_m^+ e^{-\mu_m+j\theta_m}\left[\frac{\bar{A}_n e^{-\alpha_n-j\omega_n}}{1-e^{-\alpha_n-\mu_m-j(\omega_n-\theta_m)}}\right.\right.$$

$$\left.-\frac{A_n e^{\alpha_n-j\omega_n}}{1-e^{\alpha_n-\mu_m-j(\omega_n-\theta_m)}}\right] e^{-\mu_m\ell+j\theta_m\ell}$$

$$+B_m^- e^{-\mu_m(L-1)} e^{\mu_m+j\theta_m}\left[\frac{\bar{A}_n e^{-\alpha_n-j\omega_n}}{1-e^{-\alpha_n+\mu_m-j(\omega_n-\theta_m)}}\right.$$

$$\left.\left.-\frac{A_n e^{\alpha_n-j\omega_n}}{1-e^{\alpha_n+\mu_m-j(\omega_n-\theta_m)}}\right] e^{\mu_m\ell+j\theta_m\ell}\right\}$$

$$+\sum_{n=1}^{N}\sum_{m=1}^{M}\left\{A_n\left[\frac{B_m^+}{1-e^{\alpha_n-\mu_m-j(\omega_n-\theta_m)}}\right.\right.$$

$$\left.+\frac{B_m^- e^{-\mu_m(L-1)}}{1-e^{\alpha_n+\mu_m-j(\omega_n-\theta_m)}}\right] e^{-\alpha_n\ell+j\omega_n\ell}$$

$$-\bar{A}_n e^{-\alpha_n L-j\omega_n L}\left[\frac{B_m^+ e^{-\mu_m L+j\theta_m L}}{1-e^{-\alpha_n-\mu_m-j(\omega_n-\theta_m)}}\right.$$

$$\left.+\frac{B_m^- e^{\mu_m+j\theta_m L}}{1-e^{-\alpha_n+\mu_m-j(\omega_n-\theta_m)}}\right] e^{\alpha_n\ell+j\omega_n\ell}$$

$$+\sum_{r=1}^{N-M}\sum_{n=1}^{N}\left\{C_r^+ J_n(\ell-r+1)\, e^{-\alpha_n|\ell-r+1|+j\omega_n(\ell-r+1)}\right.$$

$$\left.+C_r^- J_n(\ell-L+r)\, e^{-\alpha_n|\ell-L+r|+j\omega_n(\ell-L+r)}\right\}$$

$$=\sum_{n=1}^{N} A_n e^{-\alpha_n\Delta+j\omega_n\Delta} e^{-\alpha_n\ell+j\omega_n\ell}$$

$$\ell=0,\ldots,L-1\ . \qquad \text{(B-4)}$$

In Eq. (B-4), $J_n(\ell)$ is defined by

$$J_n(\ell) \equiv A_n, \qquad 0 \leqslant \ell$$

and

$$J_n(\ell) \equiv \bar{A}_n, \qquad \ell < 0 \ .$$

As noted above, it is tacitly assumed for the present that $N > M$. The case $N = M$ will be subsequently discussed and the case $N < M$ can be treated by a straightforward extension of the methods discussed here.

Equation (B-4) may be simplified considerably by first noting that the coefficients multiplying the exponentials, $\exp(\pm \mu_m \ell + j\theta_m \ell)$, must vanish, i.e.,

$$\sum_{n=1}^{N} \left[\frac{\bar{A}_n e^{-\alpha_n - j\omega_n}}{1 - e^{-\alpha_n - \mu_m - j(\omega_n - \theta_m)}} - \frac{A_n e^{\alpha_n - j\omega_n}}{1 - e^{\alpha_n - \mu_m - j(\omega_n - \theta_m)}} \right] = 0 \ , \qquad \text{(B-5a)}$$

and

$$\sum_{n=1}^{N} \left[\frac{\bar{A}_n e^{-\alpha_n - j\omega_n}}{1 - e^{-\alpha_n + \mu_m - j(\omega_n - \theta_m)}} - \frac{A_n e^{\alpha_n - j\omega_n}}{1 - e^{\alpha_n + \mu_m - j(\omega_n - \theta_m)}} \right] = 0 \ . \qquad \text{(B-5b)}$$

The validity of Eq. (B-5) can be simply established by first forming the z-transform of $\phi_{xx}(k)$ as given by Eq. (B-2), i.e.,

$$\begin{aligned} S_{xx}(z) &= \sum_{n=1}^{N} \left[\sum_{k=-\infty}^{-1} \bar{A}_n e^{\alpha_n k + j\omega_n k} z^{-k} + \sum_{k=0}^{\infty} A_n e^{-\alpha_n k + j\omega_n k} z^{-k} \right] \\ &= \sum_{n=1}^{N} \left[\frac{\bar{A}_n e^{-\alpha_n - j\omega_n} z}{1 - e^{-\alpha_n - j\omega_n} z} + \frac{A_n}{1 - e^{-\alpha_n + j\omega_n} z^{-1}} \right] \\ &= z \sum_{n=1}^{N} \left[\frac{\bar{A}_n e^{-\alpha_n - j\omega_n}}{1 - e^{-\alpha_n - j\omega_n} z} - \frac{A_n e^{\alpha_n - j\omega_n}}{1 - e^{\alpha_n - j\omega_n} z} \right] . \end{aligned} \qquad \text{(B-6)}$$

Equations (B-5a) and (B-5b) are now established by evaluating $S_{xx}(z)$ given by Eq. (B-6) at $z = \exp(\pm \mu_m + j\theta_m)$ and noting that the result must vanish (from Eq. (A-2)).

Another important simplification of Eq. (B-4) results by observing that the absolute value signs in the arguments of the exponentials on the left hand side of Eq. (B-4) may be removed. This can be seen by first noting that

$$J_n(\ell-r+1)\, e^{-\alpha_n|\ell-r+1|+j\omega_n(\ell-r+1)}$$

$$= A_n\, e^{-\alpha_n(\ell-r+1)+j\omega_n(\ell-r+1)}$$

$$+ \sum_{p=1}^{r-1} \left(\bar{A}_n\, e^{-\alpha_n p - j\omega_n p} - A_n\, e^{\alpha_n p - j\omega_n p} \right) \delta(\ell-r+1+p)$$

$$0 < \ell < L-1 \ , \qquad \text{(B-7a)}$$

and

$$J_n(\ell+r-L)\, e^{-\alpha_n|\ell+r-L|+j\omega_n(\ell+r-L)}$$

$$= \bar{A}_n\, e^{j\omega_n(\ell+r-L)+\alpha_n(\ell+r-L)}$$

$$+ \sum_{p=0}^{r-1} \left(A_n\, e^{-\alpha_n p + j\omega_n p} - \bar{A}_n\, e^{\alpha_n p + j\omega_n p} \right) \delta(\ell+r-L-p)$$

$$0 \leq \ell \leq L-1 \ . \qquad \text{(B-7b)}$$

The summation appearing in Eq. (B-7a) vanishes, by definition, when r=1. Substituting Eq. (B-7) into Eq. (B-4) gives rise to terms involving the delta functions which appear on the right hand side of Eq. (B-7). Specifically, these terms are given by:

$$\sum_{r=1}^{N-M} C_r^+ \sum_{p=1}^{r-1} \delta(\ell-r+1+p) \sum_{n=1}^{N} \left(\bar{A}_n\, e^{-\alpha_n p - j\omega_n p} - A_n\, e^{\alpha_n p - j\omega_n p} \right)$$

$$0 \leq \ell < L-1 \ , \qquad \text{(B-8a)}$$

and

$$\sum_{r=1}^{N-M} C_r^- \sum_{p=0}^{r-1} \delta(\ell+r-L-p) \sum_{n=1}^{N} \left(A_n\, e^{-\alpha_n p + j\omega_n p} - \bar{A}_n\, e^{\alpha_n p + j\omega_n p} \right)$$

$$0 \leq \ell \leq L-1 \ . \qquad \text{(B-8b)}$$

It is now shown that Eqs. (B-8a) and (B-8b) vanish. To show this, we will show, equivalently, that:

$$\sum_{n=1}^{N} A_n\, e^{-\alpha_n p + j\omega_n p} = \sum_{n=1}^{N} \bar{A}_n\, e^{\alpha_n p + j\omega_n p}$$

$$0 \leq p \leq N-M-1 \ . \qquad \text{(B-9)}$$

Equation (B-9) can be established by a conventional residue argument. Note from Eqs. (B-2) and (A-2) that for $p \geq 0$:

$$\sum_{n=1}^{N} A_n e^{-\alpha_n p + j\omega_n p}$$

$$= \frac{B}{2\pi j} \oint_{|z|=1} dz\, z^{p+N-M-1} \cdot \left\{ \frac{\prod_{m=1}^{M} \left(z - e^{-\mu_m + j\theta_m}\right)\left(z - e^{\mu_m + j\theta_m}\right)}{\prod_{n=1}^{N} \left(z - e^{-\alpha_n + j\omega_n}\right)\left(z - e^{\alpha_n + j\omega_n}\right)} \right\}. \qquad \text{(B-10)}$$

The constant, B, in Eq. (B-10) is given by Eq. (B-3b). The integral in Eq. (B-10) over the unit circle is equal to an integral over a large circle $|z| = R$ ($R > \max(e^{\alpha_n})$) minus the residue contributions at $z_n = \exp(\alpha_n + j\omega_n)$. However, when $0 \leq p \leq N-M-1$, the integral over the large circle vanishes (which can be seen by letting $(R \to \infty)$) and the only contributions to the integral in Eq. (B-10) are the residue contributions at $z_n = \exp(\alpha_n + j\omega_n)$. However, these contributions give, precisely, the right hand side of Eq. (B-9) and therefore, Eq. (B-9) is established.

Substituting Eqs. (B-5) and (B-7) into Eq. (B-4) and using the result given by Eq. (B-9) leads to the following relations:

$$\sum_{n=1}^{N} \sum_{m=1}^{M} \left\{ A_n \left[\frac{B_m^+}{1 - e^{\alpha_n - \mu_m - j(\omega_n - \theta_m)}} + \frac{B_m^- e^{-\mu_m (L-1)}}{1 - e^{\alpha_n + \mu_m - j(\omega_n - \theta_m)}} \right] e^{-\alpha_n \ell + j\omega_n \ell} \right.$$

$$- \bar{A}_n e^{-\alpha_n L - j\omega_n L} \left[\frac{B_m^+ e^{-\mu_m L + j\theta_m L}}{1 - e^{-\alpha_n - \mu_m - j(\omega_n - \theta_m)}} \right.$$

$$\left. \left. + \frac{B_m^- e^{\mu_m + j\theta_m L}}{1 - e^{-\alpha_n + \mu_m - j(\omega_n - \theta_m)}} \right] e^{\alpha_n \ell + j\omega_n \ell} \right\}$$

$$+ \sum_{r=1}^{N-M} \sum_{n=1}^{N} \left\{ C_r^+ A_n e^{-\alpha_n(\ell-r+1) + j\omega_n(\ell-r+1)} \right.$$

$$\left. + C_r^- \bar{A}_n e^{\alpha_n(\ell+r-L) + j\omega_n(\ell+r-L)} \right\} = \sum_{n=1}^{N} A_n e^{-\alpha_n(\Delta+\ell) + j\omega_n(\Delta+\ell)}$$

$$0 \leq \ell \leq L-1 \ . \qquad \text{(B-11)}$$

The constants $B_m^{\pm}$ and $C_r^{\pm}$ can now be determined by equating coefficients of the exponentials, $\exp(\pm\alpha_n \ell + j\omega_n \ell)$, in Eq. (B-11). The desired relations for the $B_m^{\pm}$, $C_r^{\pm}$ are given by:

$$\sum_{m=1}^{M} \left\{ \frac{B_m^+}{1 - e^{\alpha_n - \mu_m - j(\omega_n - \theta_m)}} + \frac{B_m^- e^{-\mu_m(L-1)}}{1 - e^{\alpha_n + \mu_m - j(\omega_n - \theta_m)}} \right\}$$

$$+ \sum_{r=1}^{N-M} C_r^+ e^{\alpha_n(r-1) - j\omega_n(r-1)} = e^{-\alpha_n \Delta + j\omega_n \Delta}$$

$$n = 1, \ldots, N \ , \qquad \text{(B-12a)}$$

and

$$\sum_{m=1}^{M} \left\{ \frac{B_m^+ e^{-\mu_m L + j\theta_m L}}{1 - e^{-\alpha_n - \mu_m - j(\omega_n - \theta_m)}} + \frac{B_m^- e^{\mu_m + j\theta_m L}}{1 - e^{-\alpha_n + \mu_m - j(\omega_n - \theta_m)}} \right\}$$

$$- \sum_{r=1}^{N-M} C_r^- e^{\alpha_n r + j\omega_n r} = 0 \qquad n = 1, \ldots, N \ . \qquad \text{(B-12b)}$$

Equations (B-12a) and (B-12b) are valid when $M < N$. The only modification which is needed when $M = N$ is to remove the summation terms involving the $C_r^{\pm}$ in Eqs. (B-12a) and (B-12b). That is, when $M = N$ only damped exponentials appear in the analytic solution for the LPF coefficients. It should be pointed out that Eq. (B-12) was originally presented in Reference [22] without derivations. Also, analogous equations to Eq. (B-12) appear in the treatment of the continuous problem and a more complete analytical discussion of equations similar to Eq. (B-12) is given in Reference [25], Chapter 8.

APPENDIX C. DEVELOPMENT OF APPROXIMATE POLE-ZERO MODELS FOR NARROWBAND PROCESSES IN ADDITIVE BROADBAND NOISE

In this Appendix, approximate rational spectrum models will be developed for narrowband processes embedded in additive broadband noise. The cases of additive uncorrelated and additive correlated noise will be analyzed in parts 1 and 2, respectively.

1. NARROWBAND PROCESSES EMBEDDED IN ADDITIVE UNCORRELATED NOISE†

For this class of inputs, the autocorrelation function may be expressed as

$$\phi_{xx}(k) = \phi_{no}(k) + \phi_s(k) \ , \tag{C-1}$$

where $\phi_{no}(k)$ and $\phi_s(k)$ represent the autocorrelation functions of the noise and signal, respectively. As discussed in Section III, the form of $\phi_s(k)$ which will be considered here is given by:

$$\phi_s(k) = \sum_{n=1}^{N} \sigma_n^2 e^{-\alpha_n |k|} \cos \omega_n k \ , \tag{C-2}$$

where σ_n^2, α_n, and ω_n represent the power, 3-dB half bandwidth, and frequency, respectively, of the n^{th} signal. For uncorrelated noise, the autocorrelation function of the noise is given by:

$$\phi_{no}(k) = \sigma_{no}^2 \delta(k) \ , \tag{C-3}$$

where σ_{no}^2 represents the noise power.

The model represented by Eq. (C-1) is a mixed autoregressive-moving average (ARMA) model with 2N AR terms and 2N MA terms. The z-transform of $\phi_{xx}(k)$ is given by:

$$\begin{aligned} S_{xx}(z) &= \sigma_{no}^2 + \sum_{n=1}^{2N} \frac{e^{-\alpha_n} \sinh \alpha_n \sigma_n^2}{\left(z - e^{-\alpha_n + j\omega_n}\right)\left(z^{-1} - e^{-\alpha_n - j\omega_n}\right)} \\ &= \sigma_{no}^2 - z \sum_{n=1}^{2N} \frac{\sigma_n^2 e^{j\omega_n} \sinh \alpha_n}{\left(z - e^{-\alpha_n + j\omega_n}\right)\left(z - e^{\alpha_n + j\omega_n}\right)} \\ &= \sigma_{no}^2 \frac{\prod_{n=1}^{2N} \left(z - e^{-\beta_n + j\psi_n}\right)\left(z - e^{\beta_n + j\psi_n}\right)}{\prod_{n=1}^{2N} \left(z - e^{-\alpha_n + j\omega_n}\right)\left(z - e^{\alpha_n + j\omega_n}\right)} \equiv \sigma_{no}^2 Q(z) \ . \end{aligned} \tag{C-4}$$

†The material presented in this section was originally presented in Reference [33].

In (C-4),

$$\alpha_{n+N} = \alpha_n \qquad \text{for} \qquad n = 1, \ldots, N \ , \tag{C-5a}$$

and

$$\omega_{n+N} = -\omega_n \qquad \text{for} \qquad n = 1, \ldots, N \ . \tag{C-5b}$$

As can be seen from Eq. (C-4), $S_{xx}(z)$ can be represented as a product of two factors. The first, σ_{no}^2, represents the flat power spectral density of the background uncorrelated noise. The second factor, $Q(z)$, is a rational function of z with poles located at the signal poles, $\exp(\pm\alpha_n + j\omega_n)$. The zeroes of $Q(z)$, $\exp(\pm\beta_n + j\psi_n)$, may be obtained by factoring $S_{xx}(z)$ in Eq. (C-4). In general, such a factorization of the spectrum is analytically tractable only for small values of N and does not provide much insight into the analytical structure of the zeroes of $Q(z)$. However, as the signal 3-dB half bandwidths, α_n, all become small enough so that the background noise spectral density, σ_{no}^2, may be closely approximated from $S_{xx}(e^{j\omega})$ between the signal frequencies (i.e., no appreciable overlap of signal spectra),† then a simple approximating expression for the zeroes of $Q(z)$ may be derived.

The assumption that the background noise may be closely approximated from $S_{xx}(e^{j\omega})$ is consistent with requiring that the poles and zeroes of $Q(z)$ occur in pairs, i.e.,

$$\left\{ e^{-\beta_n + j\psi_n} \ , \ e^{-\alpha_n + j\omega_n} \right\} \qquad n = 1, \ldots, 2N \ , \tag{C-6a}$$

and

$$\left\{ e^{\beta_n + j\psi_n} \ , \ e^{\alpha_n + j\omega_n} \right\} \qquad n = 1, \ldots, 2N \ , \tag{C-6b}$$

and that the distance between each member of the pair in Eq. (C-6) is very small.

Making this assumption, we can now obtain an approximate expression for the zeroes of $Q(z)$. From Eqs. (C-1) and (C-4), we have:

$$\phi_{xx}(k) = \frac{1}{2\pi j} \oint_{|z|=1} \sigma_{no}^2 \, Q(z) \, z^{k-1} \, dz \ .$$

Using Eq. (C-6) we obtain the following expression for $\phi_{xx}(k)$:

$$\phi_{xx}(k) = \sigma_{no}^2 \left\{ Q(0)\,\delta(k) + \sum_{n=1}^{2N} \frac{\left(e^{-\alpha_n + j\omega_n} - e^{-\beta_n + j\psi_n} \right)\left(e^{-\alpha_n + j\omega_n} - e^{\beta_n + j\psi_n} \right)}{e^{-\alpha_n + j\omega_n} - e^{\alpha_n + j\omega_n}} \right.$$
$$\left. \cdot \, Q_n\left(e^{-\alpha_n + j\omega_n} \right) e^{-\alpha_n(k-1) + j\omega_n(k-1)} \right\}$$
$$k \geq 0 \ . \tag{C-7}$$

†Note that no appreciable signal spectra overlap also implies that the signal frequencies, ω_n, are sufficiently greater than zero so that there is no overlap between the positive and negative frequency components of the signals.

In Eq. (C-7), $Q_n(z)$ is defined as

$$Q_n(z) \equiv \prod_{\substack{\ell=1 \\ \ell \neq n}}^{2N} \frac{\left(z - e^{-\beta_\ell + j\psi_\ell}\right)\left(z - e^{\beta_\ell + j\psi_\ell}\right)}{\left(z - e^{-\alpha_\ell + j\omega_\ell}\right)\left(z - e^{\alpha_\ell + j\omega_\ell}\right)} \quad . \tag{C-8}$$

Under the assumptions of small α_n, and little signal overlap, we have approximately that $Q(0) = 1$ and

$$Q_n\left(e^{-\alpha_n + j\omega_n}\right) = 1 \quad . \tag{C-9}$$

Therefore, equating Eqs. (C-7) and (C-1) and using Eq. (C-9), we obtain the following approximations for β_n and ψ_n:

$$\psi_n = \omega_n \quad , \; n = 1, \ldots, 2N \quad , \tag{C-10a}$$

$$\beta_n = \cosh^{-1}\left\{\cosh \alpha_n + \frac{1}{2} SNR_n \sinh \alpha_n\right\} \quad ,$$

and

$$\beta_{n+N} = \beta_n \qquad \text{for} \qquad n=1, \ldots, N \quad . \tag{C-10b}$$

In Eq. (C-10), $SNR_n = \sigma_n^2/\sigma_{no}^2$ is the signal-to-noise ratio of the n^{th} signal.

Equation (C-10) shows that in the limit of small signal bandwidths, the zeroes of $Q(z)$ are displaced slightly back along radial lines from the signal pole locations. As the $\alpha_n \to 0$, both the zeroes and the poles approach the unit circle. This implies that in the limit of zero signal bandwidths (i.e., sinusoids in white noise) the appropriate time series model for the process represented by Eq. (C-1) is an ARMA model of order (2N, 2N) with identical AR and MA terms. This limiting result was also derived using a difference equation approach in Reference [32].

The approximations expressed by Eq. (C-10) become increasingly accurate as the distance between each member of the pole-zero pair in Eq. (C-6) becomes small, i.e., when

$$\cosh^{-1}\left\{\cosh \alpha_n + \frac{1}{2} SNR_n \sinh \alpha_n\right\} - \alpha_n \approx 0 \, . \tag{C-11a}$$

For small α_n (with SNR_n fixed), Eq. (C-11a) reduces to (from Eq. (15))

$$\sqrt{SNR_n \, \alpha_n} \approx 0 \quad . \tag{C-11b}$$

Vice versa, for small SNR_n (with α_n fixed) Eq. (C-11a) reduces to (from Eq. (14))

$$SNR_n/2 \approx 0 \quad . \tag{C-11c}$$

Note that the actual values of the differences, $\beta_n - \alpha_n$, which are required for a desired accuracy of the approximations given by Eq. (C-10) will depend on the frequency separations of the signals. This is because for fixed values of α_n and β_n, the approximation expressed by Eq. (C-9) will become worse as the signal frequency separations decrease, as is seen from Eq. (C-8). In this case, there will be appreciable signal spectra overlap and the approximations expressed by Eq. (C-10) will become invalid.

2. NARROWBAND PROCESSES EMBEDDED IN ADDITIVE CORRELATED NOISE

In this section, we will assume that the z-transform of the autocorrelation function of the input, $S_{xx}(z)$, can be represented as follows:

$$S_{xx}(z) = S_{no}(z) + S_s(z) \ , \tag{C-12}$$

where $S_{no}(z)$ is the z-transform of the noise autocorrelation function. As discussed in Section III, it will be assumed that $S_{no}(z)$ can be expressed as a rational function of z:

$$S_{no}(z) = \sigma_{no}^2 \frac{\prod_{m=1}^{M_o} \left(z - e^{-\mu'_m + j\theta'_m} \right) \left(z^{-1} - e^{-\mu'_m - j\theta'_m} \right)}{\prod_{n=1}^{N_o} \left(z - e^{-\alpha'_n + j\omega'_n} \right) \left(z^{-1} - e^{-\alpha'_n - j\omega'_n} \right)} \ , \tag{C-13}$$

where σ_{no}^2, μ'_m, and α'_n are non-zero, positive real constants and

$$-\pi \leq \omega'_n, \theta'_m \leq \pi \ , \text{ for all m,n} \ .$$

Also, in Eq. (C-12) $S_s(z)$ represents the z-transform of the signal autocorrelation function and can be obtained from Eq. (C-4), i.e.,

$$S_s(z) = \sum_{n=1}^{2N} \frac{e^{-\alpha_n} \sinh \alpha_n \, \sigma_n^2}{\left(z - e^{-\alpha_n + j\omega_n} \right) \left(z^{-1} - e^{-\alpha_n - j\omega_n} \right)} \ . \tag{C-14}$$

Based on the discussion presented in Section C-1, it is expected that a reasonable approximation for $S_{xx}(z)$ under the assumption of small α_n (little signal overlap) will be given by:

$$S_{xx}(z) \cong S_{no}(z) \, Q(z) \ . \tag{C-15}$$

Equation (C-15) is directly analogous to Eq. (C-4) with σ_{no}^2 replaced by $S_{no}(z)$. Also, the function Q(z) in Eq. (C-15) is assumed to be represented by a rational function of z as in Eq. (C-4) with 2N poles located at the signal poles, $\exp(\pm\alpha_n + j\omega_n)$, and 2N zeroes which are represented by $\exp(\pm\beta_n + j\psi_n)$. Equation (C-15) implies that the input process can be approximated by an ARMA process with $2N + M_o$ zeroes and $2N + N_o$ poles. It is important to point out that this is only an approximation since the order of the exact ARMA model which represents the input process will, in general, be different (as can be seen from Eqs. (C-12) through (C-14)). However, as the $\alpha_n \to 0$, Eq. (C-15) will provide an increasingly accurate model as will be shown below.

Carrying out the integral evaluation for $\phi_{xx}(k)$ as in Eq. (C-7) with $S_{xx}(z)$ given by Eq. (C-15) gives:

$$\phi_{xx}(k) = \frac{1}{2\pi j} \oint_{|z|=1} S_{no}(z)\, Q(z)\, z^{k-1}\, dz$$

$$= \tilde{\phi}_{no}(k) + \sum_{n=1}^{2N} \frac{\left(e^{-\alpha_n + j\omega_n} - e^{-\beta_n + j\psi_n}\right)\left(e^{-\alpha_n + j\omega_n} - e^{\beta_n + j\psi_n}\right)}{e^{-\alpha_n + j\omega_n} - e^{\alpha_n + j\omega_n}}$$

$$\cdot Q_n\left(e^{-\alpha_n + j\omega_n}\right) S_{no}\left(e^{-\alpha_n + j\omega_n}\right) e^{(-\alpha_n + j\omega_n)(k-1)}$$

$$k \geq 0 \ . \qquad \text{(C-16)}$$

In Eq. (C-16), $Q_n(z)$ is defined as in Eq. (C-8) and $\tilde{\phi}_{no}(k)$ represents the contribution to the integral which arises from the poles of the function $z^{k-1} S_{no}(z)$. Assuming that these poles are sufficiently separated from the signal poles so that $Q(0) \approx 1$ and

$$Q\left(e^{-\alpha'_n + j\omega'_n}\right) \approx 1 \qquad n = 1, \ldots, N_o \ , \qquad \text{(C-17)}$$

then $\tilde{\phi}_{no}(k)$ will approximately equal the true autocorrelation function of the noise, $\phi_{no}(k)$. Also, it is seen that the contribution from the signal poles in Eq. (C-16) is practically identical to that for the white noise case (see Eq. (C-7)). Their main difference is the *factor*, $S_{no}(e^{-\alpha_n + j\omega_n})$, *in* Eq. (C-16). This quantity can be approximated for small α_n as follows:

$$S_{no}\left(e^{-\alpha_n + j\omega_n}\right) \approx S_{no}\left(e^{j\omega_n}\right)\left\{1 - \alpha_n e^{j\omega_n} S'_{no}\left(e^{j\omega_n}\right)/S_{no}\left(e^{j\omega_n}\right)\right\} \ . \qquad \text{(C-18)}$$

Therefore, provided

$$\alpha_n \left|S'_{no}\left(e^{j\omega_n}\right)/S_{no}\left(e^{j\omega_n}\right)\right| \ll 1 \ , \qquad \text{(C-19)}$$

then an approximation for the β_n and ψ_n can be obtained in direct analogy with Eq. (C-10), i.e.,

$$\psi_n = \omega_n \ , \ n = 1, \ldots, 2N \ , \qquad \text{(C-20a)}$$

$$\beta_n = \cosh^{-1}\left\{\cosh \alpha_n + \frac{1}{2} SNR_n \sinh \alpha_n\right\} \ ,$$

and

$$\beta_{n+N} = \beta_n \text{ for } n = 1, \ldots, N \ . \qquad \text{(C-20b)}$$

In Eq. (C-20), $SNR_n \equiv \sigma_n^2/S_{no}(e^{j\omega_n})$ and is the signal-to-noise spectral density ratio at the n^{th} signal. Note that Eq. (C-19) will be satisfied either in the limit of small signal bandwidths or provided the background noise spectral density is not varying too rapidly in the vicinity of the signal. If this is not the case, then the signal zeroes, $\exp(\pm\beta_n + j\psi_n)$, will not, in general, lie on the same radials as the signal poles.

APPENDIX D. TREATMENT OF THE COEFFICIENT EQUATIONS FOR NARROWBAND PROCESSES EMBEDDED IN BROADBAND NOISE

In this Appendix, the coefficient Eqs. (5) and (6) will be analyzed for inputs consisting of narrowband signal processes embedded in additive broadband noise. It will be assumed, as in Section III, that the autocorrelation function of the input is given by Eq. (10), the z-transform of the noise autocorrelation function is given by Eq. (11), and the zeroes of $S_{xx}(z)$ are approximated by Eq. (13). The impulse response of the discrete LPF will be expressed as follows:

$$w^*(k) = h_s(k) + h_{no}(k) \qquad k = 0, 1, \ldots, L-1 \ , \tag{D-1}$$

where $h_s(k)$ is given by

$$h_s(k) = \sum_{n=1}^{2N} \left\{ B_n^{+s} e^{-\beta_n k + j\omega_n k} + B_n^{-s} e^{-\beta_n (L-1-k) + j\omega_n k} \right\} , \tag{D-2}$$

and $h_{no}(k)$ is given by

$$h_{no}(k) = \sum_{m=1}^{M_o} \left\{ B_m^{+0} e^{-\mu'_m k + j\theta'_m k} + B_m^{-0} e^{-\mu'_m (L-1-k) + j\theta'_m k} \right\} + \sum_{r=1}^{N_o - M_o} \left\{ C_r^{+0} \delta(k-r+1) + C_r^{-0} \delta(k+r-L) \right\} . \tag{D-3}$$

The constants $B_n^{\pm s}$, $B_m^{\pm 0}$, and $C_r^{\pm 0}$ can be determined from the coefficient Eqs. (5) and (6). A general treatment of these equations is quite involved when there is appreciable coupling between the different signal amplitudes, $B_n^{\pm s}$. However, when all of the signal bandwidths are quite small and provided L is large enough, some useful approximations for the $B_n^{\pm s}$ can be obtained. In this Appendix, we will treat Eqs. (5) and (6) under two limiting approximations. First, we will consider the limit of large L such that

$$L \gg 1/\mu'_m \ , \ m = 1, \ldots, M_o \tag{D-4a}$$

and

$$L \gg 1/\beta_n \ , \ n = 1, \ldots, 2N \ . \tag{D-4b}$$

Then, we will consider the limit of small signal bandwidths such that

$$\beta_n \ll 1/L \text{ for all } n = 1, \ldots, 2N \ . \tag{D-5}$$

LIMIT OF LARGE L

As discussed in Section II, as $L \to \infty$ so that Eq. (D-4) is valid, all of the reflection amplitudes, B_n^{-s}, B_m^{-0}, and C_r^{-0} approach zero. From Eq. (5) it is seen that in this limiting case, the B_n^{+s} satisfy

$$\frac{B_n^{+s}}{1 - e^{\alpha_n - \beta_n}} + \sum_{\substack{m=1 \\ m \neq n}}^{2N} \frac{B_m^{+s}}{1 - e^{\alpha_n - \beta_m - j(\omega_n - \omega_m)}}$$

$$+ \sum_{m=1}^{M_o} \frac{B_m^{+0}}{1 - e^{\alpha_n - \mu'_m - j(\omega_n - \theta'_m)}}$$

$$+ \sum_{r=1}^{N_o - M_o} C_r^{+0} e^{\alpha_n (r-1) - j\omega_n (r-1)} = e^{-\alpha_n \Delta + j\omega_n \Delta}$$

$$n = 1, \ldots, 2N \ , \qquad \text{(D-6)}$$

where in Eq. (D-6), $\alpha_{n+N} \equiv \alpha_n$ ($n = 1, \ldots, N$). When the differences, $\beta_n - \alpha_n$, are all very small, then we can make the approximation:

$$1 - e^{\alpha_n - \beta_n} \approx \beta_n - \alpha_n \ll 1 \qquad n = 1, \ldots, 2N \ . \qquad \text{(D-7)}$$

As seen from Eqs. (13) through (15), Eq. (D-7) becomes valid either in the limit of small signal bandwidths or small SNR_n. Also, provided the signals are all separated far enough apart in frequency so that:

$$\beta_n - \alpha_n \ll \left| 1 - e^{\alpha_n - \beta_m - j(\omega_n - \omega_m)} \right| \qquad \text{(D-8)}$$

$$\text{for } n, m = 1, \ldots, 2N \ (n \neq m) \ ,$$

then the coefficient matrix which multiplies the column vector with components B_n^{+s} in Eq. (D-6) becomes approximately diagonal. Under this approximation, the coupling between the B_n^{+s} in Eq. (D-6) vanishes and we have the following approximation:

$$B_n^{+s} \approx (\beta_n - \alpha_n) \Bigg\{ e^{-\alpha_n \Delta + j\omega_n \Delta}$$

$$- \sum_{m=1}^{M_o} \frac{B_m^{+0}}{1 - e^{\alpha_n - \mu'_m - j(\omega_n - \theta'_m)}}$$

$$- \sum_{r=1}^{N_o - M_o} C_r^{+0} e^{\alpha_n (r-1) - j\omega_n (r-1)} \Bigg\}$$

$$n = 1, \ldots, 2N \ . \qquad \text{(D-9)}$$

We now examine the additional relations which the B_m^{+0} and C_r^{+0} must obey (from Eq. (5) with $L \to \infty$):

$$\sum_{m=1}^{M_o} \frac{B_m^{+0}}{1 - e^{\alpha'_n - \mu'_m - j(\omega'_n - \theta'_m)}} + \sum_{r=1}^{N_o - M_o} C_r^{+0}\, e^{\alpha'_n (r-1) - j\omega'_n (r-1)} + \sum_{m=1}^{2N} \frac{B_m^{+s}}{1 - e^{\alpha'_n - \beta_m - j(\omega'_n - \omega_m)}} = e^{-\alpha'_n \Delta + j\omega'_n \Delta} \qquad \text{(D-10)}$$

$$n = 1, \ldots, N_o \ .$$

Equation (D-10) shows that provided the background noise is decorrelated, i.e.,

$$e^{-\alpha'_n \Delta} \approx 0 \ , \text{ for all } n = 1, \ldots, N_o \ , \qquad \text{(D-11)}$$

then the constants B_m^{+0} and C_r^{+0} will be linearly related to the amplitudes B_m^{+s}. By substituting Eq. (D-9) into Eq. (D-10) for the B_m^{+s} it is seen that the constants B_m^{+0} and C_r^{+0} are of order $(\beta_n - \alpha_n)$ for small values of $(\beta_n - \alpha_n)$. *Therefore, if there is little signal decorrelation,* i.e.,

$$e^{-\alpha_n \Delta} \approx 1 \ , \text{ for all } n = 1, \ldots, N \ , \qquad \text{(D-12)}$$

and provided Eq. (D-7) holds, then from Eq. (D-9) it is seen that:

$$B_n^{+s} \approx (\beta_n - \alpha_n)\, e^{-\alpha_n \Delta + j\omega_n \Delta} \qquad n = 1, \ldots, 2N \ . \qquad \text{(D-13)}$$

Equation (D-13) is the desired approximation for the B_n^{+s} in the limit of large L.

LIMIT OF SMALL SIGNAL BANDWIDTHS

As can be seen from Eq. (D-2), as $\beta_n L \to 0$, $h_s(k)$ is approximately given by

$$h_s(k) \cong \sum_{n=1}^{2N} \left\{ A_n e^{j\omega_n k} - G_n \beta_n k e^{j\omega_n k} \right\}$$

$$0 \leq k \leq L-1 \ , \qquad \text{(D-14a)}$$

where

$$A_n = B_n^{+s} + B_n^{-s} \qquad \text{(D-14b)}$$

and

$$G_n = B_n^{+s} - B_n^{-s} \quad . \tag{D-14c}$$

As will be shown below, the G_n in Eq. (D-14a) will approach zero as the α_n approach zero. The method which is used in this section for analyzing Eqs. (5) and (6) consists of separating the $2N + N_o$ equations in Eq. (5) and the $2N + N_o$ equations in Eq. (6) into $2N$ equations for the amplitudes, A_n, and $2N_o$ equations for the amplitudes $B_m^{\pm 0}$ and $C_r^{\pm 0}$. As will be seen, these two sets of equations will be coupled together in analogy with Eqs. (D-6) and (D-10).

Using Eqs. (D-14b) and (D-14c) in the coefficient Eqs. (5) and (6), we can express the equations for the $B_n^{\pm s}$ in terms of the A_n and G_n (in the limit as all of the $\beta_n L \to 0$):†

$$\frac{1}{2}\left\{\sum_{\substack{m=1\\ m\neq n}}^{2N} \frac{1}{1-e^{-j(\omega_n-\omega_m)}}\left[A_m\left(2-\beta_m(L-1)\right)+G_m\beta_m(L-1)\right]\right\}$$

$$+\frac{1}{2}A_n\frac{\left(2\alpha_n+\beta_n^2(L-1)\right)}{\beta_n^2-\alpha_n^2}+\frac{1}{2}\frac{G_n\left(2\beta_n-\beta_n^2(L-1)\right)}{\beta_n^2-\alpha_n^2}$$

$$+\sum_{m=1}^{M_o}\left\{\frac{B_m^{+0}}{1-e^{\alpha_n-\mu'_m-j(\omega_n-\theta'_m)}}+\frac{B_m^{-0}\,e^{-\mu'_m(L-1)}}{1-e^{\alpha_n+\mu'_m-j(\omega_n-\theta'_m)}}\right\}$$

$$+\sum_{r=1}^{N_o-M_o} C_r^{+0}\,e^{\alpha_n(r-1)-j\omega_n(r-1)} = e^{-\alpha_n\Delta+j\omega_n\Delta}$$

$$n = 1,\ldots,2N \ , \tag{D-15a}$$

and

$$\frac{1}{2}\left\{\sum_{\substack{m=1\\ m\neq n}}^{2N} \frac{e^{-j(\omega_n-\omega_m)L}}{1-e^{-j(\omega_n-\omega_m)}}\left[A_m(2-\beta_m(L-1)-G_m(\beta_m(L+1))\right]\right\}$$

$$-\frac{1}{2}A_n\frac{\left(2\alpha_n+\beta_n^2(L+1)\right)}{\beta_n^2-\alpha_n^2}+\frac{1}{2}G_n\frac{\left(2\beta_n-\beta_n^2(L-1)\right)}{\beta_n^2-\alpha_n^2}$$

† In deriving Eq. (D-15) we assume that $\beta_n L$ is small enough that $\exp(\pm\beta_n L) \approx 1 \pm \beta_n L$. Also, the products $\alpha_n\beta_n$ are neglected in comparison with the terms β_n^2 (which is valid as $\alpha_n \to 0$ (see Eq. (15)).

$$+ e^{-j\omega_n L} \sum_{m=1}^{M} \left\{ \frac{B_m^{+0} e^{-\mu'_m L + j\theta'_m L}}{1 - e^{-\alpha_n - \mu'_m - j(\omega_n - \theta'_m)}} \right.$$

$$\left. + \frac{B_m^{-0} e^{\mu'_m + j\theta'_m L}}{1 - e^{-\alpha_n + \mu'_m - j(\omega_n - \theta'_m)}} \right\}$$

$$- \sum_{r=1}^{N_o - M_o} C_r^{-0} e^{\alpha_n r - j\omega_n (L-r)} = 0 \qquad \text{(D-15b)}$$

$$n = 1, \ldots, 2N \ .$$

Notice that the G_m terms which appear in the summations in Eq. (D-15) are all multiplied by the β_m (which approach zero as α_m approaches zero). Notice also that the term,

$$\frac{1}{2} G_n \frac{\left(2\beta_n - \beta_n^2 (L-1) \right)}{\beta_n^2 - \alpha_n^2} \ ,$$

appears on the left hand sides of Eqs. (D-15a) and (D-15b). Transposing this term to the right hand side of Eq. (D-15b), substituting the result into Eq. (D-15a), and letting the $\alpha_n \to 0$ (with the β_n approximated by Eq. (15)) results in the following limiting equations for the A_n (which are independent of the G_n, β_n, and α_n):

$$\frac{LSNR_n/2+1}{SNR_n/2} A_n + \sum_{\substack{m=1 \\ m \neq n}}^{2N} \frac{A_m \left(1 - e^{-j(\omega_n - \omega_m)L} \right)}{1 - e^{-j(\omega_n - \omega_m)}} = e^{j\omega_n \Delta}$$

$$- \sum_{m=1}^{M_o} \left\{ B_m^{+0} \frac{\left(1 - e^{-\mu'_m L - j(\omega_n - \theta'_m)L} \right)}{1 - e^{-\mu'_m - j(\omega_n - \theta'_m)}} \right.$$

$$\left. + B_m^{-0} \frac{\left(e^{-\mu'_m (L-1)} - e^{\mu'_m - j(\omega_n - \theta'_m)L} \right)}{1 - e^{\mu'_m - j(\omega_n - \theta'_m)}} \right\}$$

$$- \sum_{r=1}^{N_o - M_o} \left\{ C_r^{+0} e^{-j\omega_n (r-1)} + C_r^{-0} e^{-j\omega_n (L-r)} \right\}$$

$$n = 1, 2, \ldots, 2N \ . \qquad \text{(D-16)}$$

Additional equations for the $B_m^{\pm 0}$, $C_r^{\pm 0}$, and the A_n can be obtained from the $2N_o$ equations of Eqs. (5) and (6) that involve the noise poles. These equations are as follows (in the limit as the $\alpha_n \to 0$):

$$\sum_{m=1}^{M_o} \left\{ \frac{B_m^{+0}}{1 - e^{\alpha'_n - \mu'_m - j(\omega'_n - \theta'_m)}} + \frac{B_m^{-0}\, e^{-\mu'_m(L-1)}}{1 - e^{\alpha'_n + \mu'_m - j(\omega'_n - \theta'_m)}} \right\}$$

$$+ \sum_{m=1}^{2N} \frac{A_m}{1 - e^{\alpha'_n - j(\omega'_n - \omega_m)}} + \sum_{r=1}^{N_o - M_o} C_r^{+0}\, e^{\alpha'_n(r-1) - j\omega'_n(r-1)}$$

$$= e^{-\alpha'_n \Delta + j\omega'_n \Delta}$$

$$n = 1, \ldots, N_o \ , \qquad \text{(D-17)}$$

and

$$\sum_{m=1}^{M_o} \left\{ \frac{B_m^{+0}\, e^{-\mu'_m L + j\theta'_m L}}{1 - e^{-\alpha'_n - \mu'_m - j(\omega'_n - \theta'_m)}} + \frac{B_m^{-0}\, e^{\mu'_m + j\theta'_m L}}{1 - e^{-\alpha'_n + \mu'_m - j(\omega'_n - \theta'_m)}} \right\}$$

$$+ \sum_{m=1}^{2N} \frac{A_m\, e^{j\omega_m L}}{1 - e^{-\alpha'_n - j(\omega'_n - \omega_m)}} - \sum_{r=1}^{N_o - M_o} C_r^{-0}\, e^{\alpha'_n r + j\omega'_n r} = 0 \ , \qquad \text{(D-18)}$$

$$n = 1, \ldots, N_o \ .$$

Note that Eqs. (D-16) through (D-18) show that as the signal bandwidths, α_n, approach zero, the A_n, $B_m^{\pm 0}$, and $C_r^{\pm 0}$ all become independent of the α_n. Therefore, from Eq. (D-15b) it is seen that the term,

$$\frac{1}{2} G_n \frac{\left(2\beta_n - \beta_n^2 (L-1)\right)}{\beta_n^2 - \alpha_n^2} \approx G_n (SNR_n \alpha_n)^{-1/2} \ ,$$

must approach a constant (independent of α_n) as all of the α_n approach zero. Therefore, G_n approaches zero as $\alpha_n \to 0$ and from Eq. (D-14) it is seen that $h_s(k)$ is given approximately by:

$$h_s(k) \approx \sum_{n=1}^{2N} A_n\, e^{j\omega_n k} \ . \qquad \text{(D-19)}$$

It should be pointed out that Eqs. (D-16) through (D-18) could also have been derived by substituting Eqs. (D-1), (D-3), and (D-19) into Eq. (1) and equating coefficients as discussed in Appendix B.

As can be seen from the left hand side of Eq. (D-16), as the quantity $(LSNR_n/2+1)/(SNR_n/2)$ becomes large, the coefficient matrix which multiplies the column vector with components A_n in Eq. (D-16) becomes approximately diagonal. Also, provided the background noise is decorrelated (D-11), then the amplitudes $B_m^{\pm 0}$ and $C_r^{\pm 0}$ will be linearly related to the A_n, as can be seen from Eqs. (D-17) and (D-18). Therefore, in analogy with the treatment of Eqs. (D-9) and (D-10) for large L, it is seen from Eqs. (D-16) through (D-18) that:

$$A_n \approx \frac{SNR_n/2}{1 + LSNR_n/2} e^{j\omega_n \Delta} \qquad n = 1, \ldots, 2N \ . \qquad \text{(D-20)}$$

Note that $(LSNR_n/2 + 1)/(SNR_n/2)$ becomes large either in the limit of large L or small SNR_n. Therefore, in either of these limits, Eq. (D-20) will provide a good approximation for the A_n.

REFERENCES

1. B. Holt, R. Houts, "Multiband FIR Digital Filter Design Algorithm for Radar Clutter Suppression," Proc. 1978 IEEE Int. Conf. on Acous., Speech, and Sig. Proc., pp. 228–231, April 10-12, 1978, Tulsa, OK.

2. N. Wiener, Extrapolation, Interpolation, and Smoothing of Stationary Time Series, With Engineering Applications, New York: Wiley, 1949.

3. B. Widrow, M. E. Hoff, Jr., "Adaptive Switching Circuits," 1960 IRE WESCON Conv. Record, pt 4, pp 96–104.

4. B. Widrow, "Adaptive Filters," in Aspects of Network and System Theory, R. Kalman and N. DeClaris, Eds, New York: Holt, Rinehart, and Winston, 1971 pp 563–587.

5. B. Widrow, et al, "Adaptive Noise Cancelling: Principles and Applications," Proc. IEEE, Vol. 63, pp 1692–1716, December 1975.

6. F. J. Harris, "A Maximum Entropy Filter," Naval Undersea Center, NUC TP 441, January 1975.

7. N. Ahmed, D. R. Hummels, M. Uhl, and D. Soldan, "A Short-Term Sequential Regression Algorithm," Proc. 1978 IEEE Int. Conf. on Acous., Speech, and Sig. Proc., pp. 123–126, April 10-12, 1978, Tulsa, OK.

8. L. J. Griffiths, "A Continuously-Adaptive Filter Implemented as a Lattice Structure," Proc. 1977 IEEE Int. Conf. on Acous., Speech, and Sig. Proc., pp. 683–686, May, 1977, Hartford, CT.

9. L. J. Griffiths, "An Adaptive Lattice Structure for Noise Cancelling Applications," Proc. 1978 IEEE Int. Conf. on Acous., Speech, and Sig. Proc., pp 87–90, April 10-12, 1978, Tulsa, OK.

10. J. Makhoul, R. Viswanathan, "Adaptive Lattice Methods for Linear Prediction, Proc. 1978 IEEE Int. Conf. on Acous., Speech, and Sig. Proc., pp. 83–86, April 10-12, 1978, Tulsa, OK.

11. J. Makhoul, "A Class of All-Zero Lattice Digital Filters: Properties and Applications," IEEE Trans. on Acous., Speech, and Sig. Proc., Vol. ASSP-26, No. 4, August 1978, pp. 304–314.

12. J. R. Zeidler, E. H. Satorius, D. M. Chabries, and H. T. Wexler, "Adaptive Enhancement of Multiple Sinusoids in Uncorrelated Noise," IEEE Trans. on Acous., Speech, and Sig. Proc., Vol. ASSP-26, No. 3, June 1978, pp. 240–254.

13. M. R. Sambur, "Adaptive Noise Cancelling for Speech Signals," IEEE Trans. on Acous., Speech, and Sig. Proc., Vol. ASSP-26, No. 5, October 1978, pp. 419–423.

14. V. V. Solodovnikov, Statistical Dynamics of Linear Automatic Control Systems, London: D. Van Nostrand Co., Ltd., 1965.

15. Ya. Z. Tsypkin, Sampling Systems Theory, Vols 1 and 2, Oxford: Pergamon Press Ltd., 1964.

16. P. D. Krut'ko, Statistical Dynamics of Sampled Data Systems, London: Iliffe Books Ltd., 1969.

17. J. Makhoul, "Linear Prediction: A Tutorial Review," Proc. IEEE, Vol. 63, pp. 561-580, April 1975.

18. T. Kailath, "A View of Three Decades of Linear Filtering Theory," IEEE Trans. on Inform. Theory, Vol. IT-20, pp 145-181, March 1974.

19. L. Zadeh, J. Ragazzini, "An Extension of Wiener's Theory of Prediction," J. Appl. Phys., Vol. 21, pp. 645-655, July 1950.

20. E. A. Robinson, Statistical Communication and Detection, New York: Hafner, 1967.

21. S. T. Alexander, R. Medaugh, M. Shensa, and J. Zeidler, "The Detection of Sinusoids in White Noise Using Adaptive Linear Prediction Filtering," NOSC TR 270, May 1978, submitted for publication.

22. E. H. Satorius, J. R. Zeidler, "Least-Mean-Square, Finite Length, Predictive Digital Filters," Proc. 1977 IEEE Int. Conf. on Acous., Speech, and Sig. Proc., pp 747-749, May 1977, Hartford, CT.

23. K. Peacock, S. Treitel, "Predictive Deconvolution: Theory and Practice," Geophysics, Vol. 34, pp 155-169, April 1969.

24. E. H. Satorius, "Adaptive Noise Cancelling and Enhancement of a Sinusoid in Uncorrelated Noise," Naval Ocean Systems Center, NOSC TR 184, December 1977.

25. J. H. Laning and R. H. Battin, Random Processes in Automatic Control, New York, McGraw-Hill, 1956.

26. A. Klinger, "The Vandermonde Matrix," Amer. Math. Monthly, Vol. 74, No. 5, 1967, pp. 557-574.

27. C. G. Cullen, Matrices and Linear Transformations, Second Edition, Addison-Wesley Publishing Co., Reading, Mass., 1972.

28. L. H. Koopmans, The Spectral Analysis of Time Series, New York: Academic Press, 1974.

29. J. Treichler, "The Spectral Line Enhancer," PhD Dissertation, Department of Electrical Engineering, Stanford University, Stanford CA, May 1977.

30. C. W. Helstrom, Statistical Theory of Signal Detection, London: Pergamon Press, 1960; 2nd ed. 1968.

31. W. Davenport, W. Root, An Introduction to Random Signals and Noise, New York: McGraw-Hill, 1958.

32. T. J. Ulrych, R. W. Clayton, "Time Series Modelling and Maximum Entropy," Phys. Earth Planet. Inter., Vol. 12, pp 188-200, 1976.

33. S. T. Alexander, E. H. Satorius, J. R. Zeidler, "Linear Prediction and Maximum Entropy Spectral Analysis of Finite Bandwidth Signals in Noise," Proc. 1978 IEEE Int. Conf. on Acous., Speech, and Sig. Proc., pp 188-191, April 10-12, 1978, Tulsa, OK.

34. J. D. Markel, A. H. Gray, Jr., Linear Prediction of Speech, Springer-Verlag, New York, 1976.

35. J. T. Rickard, J. R. Zeidler, "Second-Order Output Statistics of the Adaptive Line Enhancer," to appear in IEEE Trans. on Acous., Speech, and Sig. Proc.

36. D. Morgan, S. Craig, "Real-Time Linear Prediction using the Least Mean Square Gradient Algorithm," IEEE Trans. Acoust., Speech, and Sig. Proc., Vol. ASSP-24, pp. 494–507, December 1976.

37. L. J. Griffiths, F. R. Smolka, L. D. Trembly, "Adaptive Deconvolution: A New Technique for Processing Time-Varying Seismic Data," Geophysics, vol. 42, June 1977, pp. 742–759.

38. R. Keeler, L. Griffiths, "Acoustic Doppler Extraction by Adaptive Linear Prediction Filtering," J. Acoust. Soc. Amer., vol. 61, pp. 1218–1227, May 1977.

39. B. Widrow, J. Glover, J. McCool, and J. Treichler, reply to letter from D. W. Tufts, Proc. IEEE (Lett.), vol. 65, pp. 171–173, Jan. 1977.